Applying the RUSLE and SEDD Equations to an Agricultural Watershed in Southwest Virginia: A Case Study in Sediment Yield Estimation Using GIS

Lindsay B. Lally

Thesis submitted to the faculty of the Virginia Polytechnic Institute and State University
in partial fulfillment of the requirements for the degree of

Master of Science In
Civil Engineering

Panayiotis Diplas (Chair)
Paolo Scardina
Madeline Schreiber

May 3, 2013
Blacksburg, Virginia

Keywords: Hydrology, RUSLE, SEDD, Stormwater Management, Sediment Yield, ArcGIS

Applying the RUSLE and SEDD Equations to an Agricultural Watershed in Southwest Virginia: A Case Study in Sediment Yield Estimation Using GIS

Lindsay B. Lally

ABSTRACT

The goal of this study is to develop a model using GIS to estimate the source and quantity of accumulated sediment in the Emory & Henry College (EHC) duck pond. Located in the Highlands of Southwest Virginia, the 1,194 acre duck pond watershed consists primarily of agricultural, forested, and low density urban land uses.

The Revised Universal Soil Loss Equation (RUSLE) and the Sediment Distributed Delivery (SEDD) prediction models were used to determine the quantity of eroded sediment and the sediment yield at the duck pond, respectively. These models require numerous computations, which were performed at the watershed scale with the aid of ArcGIS software. In ArcGIS the watershed was broken into a raster grid of approximately 5,200 discrete 100 foot by 100 foot grid cells.

The resulting watershed erosion model identified two main sources of sediment: a cluster of farms relatively close to and east of the duck pond, and a harvested timber site north of the duck pond. The model predicted that 1,076 tons of sediment are delivered *into* the duck pond annually.

The estimated sediment yield was then compared to the estimated amount deposited between October 2011 and September 2012, as measured by a topographic survey. The model prediction was found to be within a factor of 6.3x of the measured value. The predicted and measured sediment yields as well as identified erosion sources can be used to develop a water quality improvement plan and to help alleviate the need for periodic dredging.

DEDICATION

I would like to dedicate this work to my husband, Evan, and our amazing little Anna. I am filled with your spirit and love.

ACKNOWLEDGEMENTS

I would like to thank Dr. Panos Diplas for supporting and encouraging my studies as well as my personal endeavors while in graduate school at Virginia Tech. I would also like to thank my committee members, Dr. Madeline Schreiber and Dr. Paolo Scardina for their guidance and enthusiasm. A special thanks is also extended to Rajan Jha and Zackary Munger for their assistance in the lab.

To my family, you make me the luckiest person in the world. Without your continued support and love none of this would be possible. From helping with data collection to babysitting to simply inquiring about my work, your assistance and support is immensely appreciated. Thank you Mom, Dad, Michael, Kathy, Mike, Meg, and Phil. And to Evan and Anna, you inspire me to be a better person.

I would like to thank Draper Aden Associates for donating services and allowing me to maintain a flexible work schedule. I greatly appreciate Mike Futrell for his eagerness in helping me with GIS. I would especially like to thank Hoppy Knighting, James Ferrell, Mickey Mullens, and Michael Sink for donating surveying expertise and time and Carolyn Howard for her understanding and patience. Thank you especially to Matt James for helping me navigate through the details - you make work fun!

My gratitude is also extended to the staff at Emory & Henry College in Emory, Virginia. Working on your beautiful campus has been a privilege.

TABLE OF CONTENTS

LIST OF FIGURES

LIST OF TABLES

Chapter 1. Introduction and Background

Emory & Henry College (the College or EHC), a small private college founded in 1836, is located in the Highlands of Southwest Virginia. The entire main campus is listed on the National Register of Historic Places. The campus duck pond, and the springs that feed it, play an important role in the College's history. However, this beloved campus amenity has fallen into disrepair and is plagued by sediment accumulation, which requires costly periodic dredging. Dredging, which cost the College approximately $30,000 in 2011, is done to decrease the flooding potential and to improve water quality. Controlling the flooding potential is particularly important because the duck pond is immediately adjacent to the Van Dyke Center and the Studio Theatre, both shown in Figure 1 (top right).

The College dredges the accumulated pond sediment biennially and seeks ways to reduce maintenance costs. The purpose of this project is to identify the sources of erosion within the watershed and to predict the annual sediment yield expected at the pond.

Several springs, which have been active since the College was founded in 1836, feed the current-day duck pond. Early in the College's history, before the invention of modern refrigeration, a spring house was constructed to harness the natural cooling capabilities of the spring water. After World War II, the spring house was demolished, and the modern-day duck pond was constructed in the Spring of 1950 (Stevenson, 1963). The spring house foundation still exists today.

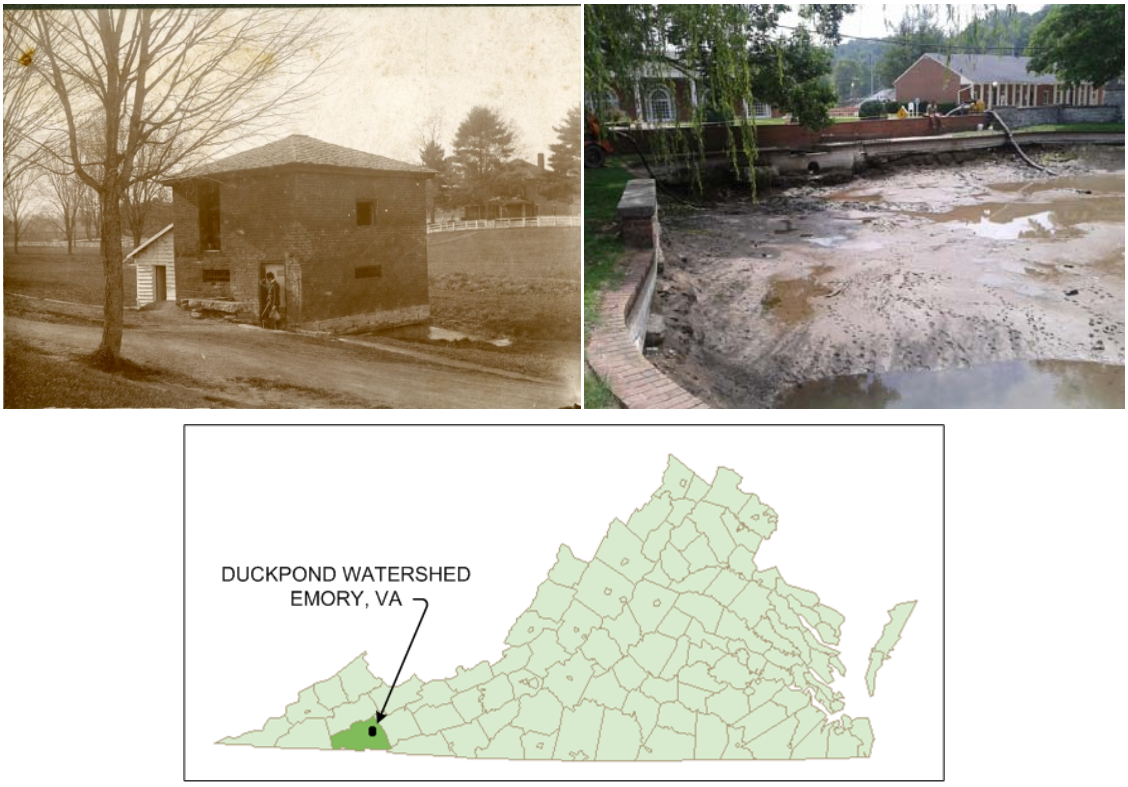

Figure 1. Emory & Henry College Duck Pond and location map: (top left) historical image of pump house - EHC image archive, (top right) image of modern-day pond, drained, (bottom) location map - Washington County, Virginia

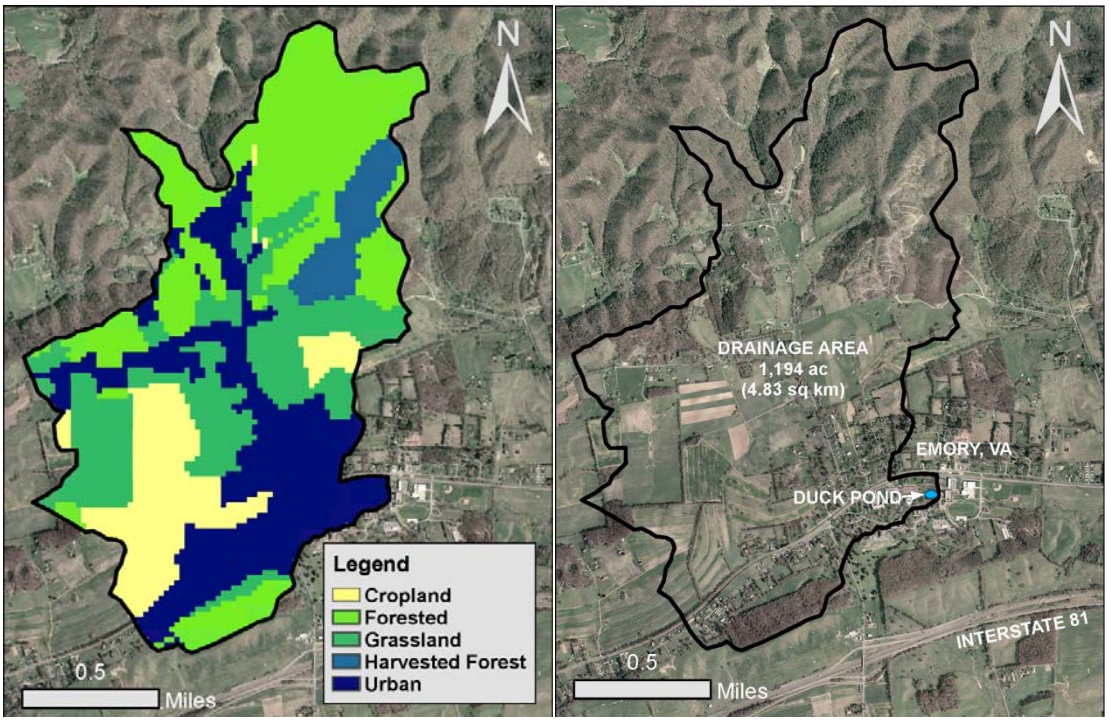

Figure 2. Watershed & land usage maps: (left) land usage by category, (right) aerial photograph [Data sources listed in Section 2.3]

The irregularly-shaped 8-ft deep pond occupies approximately 0.26 acres. The pond is the site of the Hall Creek springhead, which eventually flows to the Middle Fork of the Holston River. The pond inlet stream is ephemeral and appears to only flow immediately after a rainfall or snowmelt event. The pond outfalls through a concrete outlet structure with a 20-in diameter circular orifice and 6 x 1-foot rectangular weir. It then flows underneath Collins Drive and the Van Dyke Center where it daylights to a recently-stabilized section of Hall Creek.

The duck pond watershed is approximately 1,194 acres consisting of 26 % low density urban land, 14 % agricultural farmland, 24 % grassland and pasture, 31 % forestland, and 5 % harvested forestland (Figure 2). The watershed lowlands consist of rolling hills with slopes ranging from 1 - 15 degrees. The highlands, in the northern portion of the watershed, are forested with slopes ranging from 15 - 32 degrees. The land cover categories and watershed boundary were delineated manually through interpretation of aerial imagery and topography. The duck pond watershed topography is shown in Figure 3.

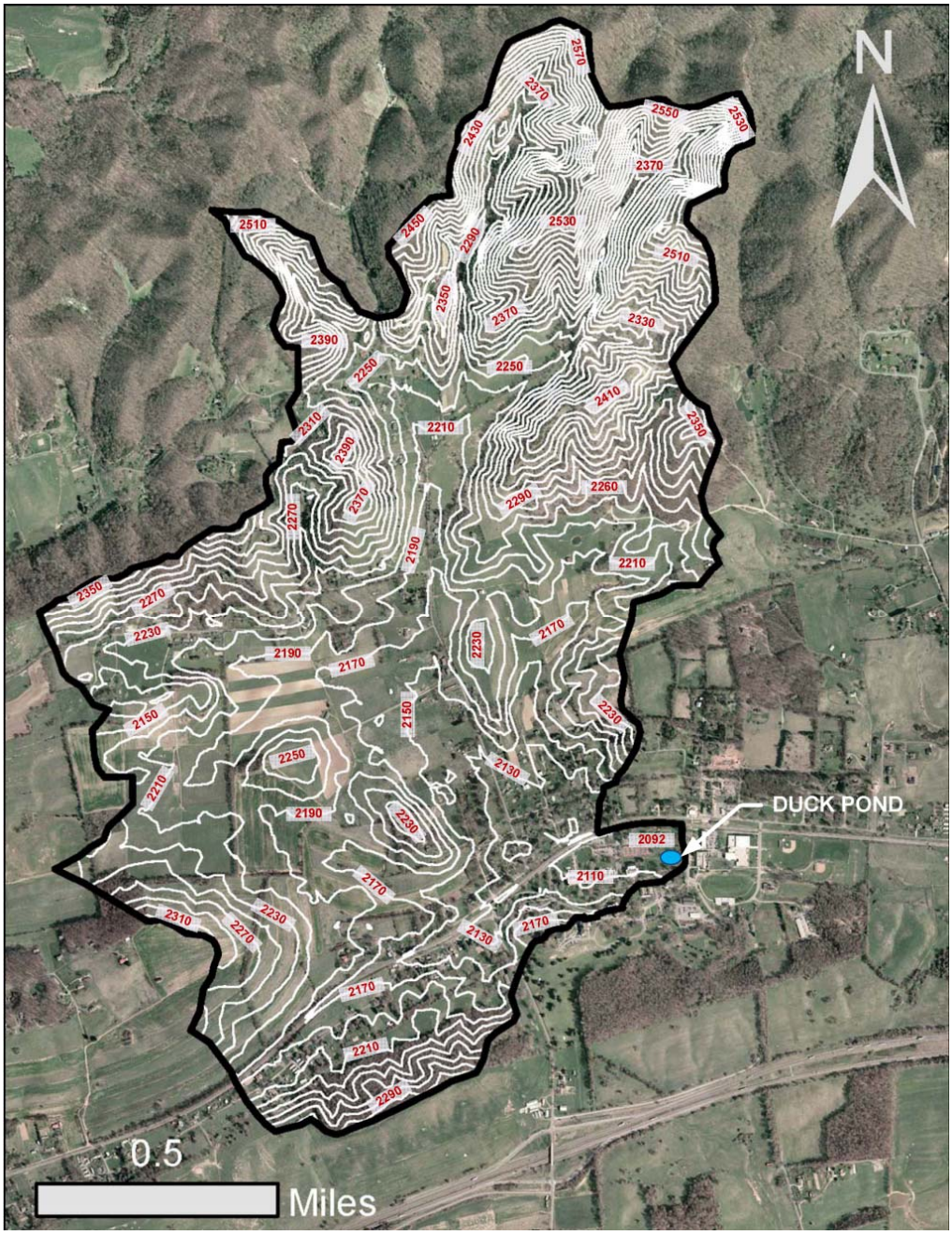

Figure 3. Duck pond watershed topographic map - 20 ft contour interval [Data sources listed in Section 2.3]

Over the past several years, the College has collected information about the condition and health of the pond. This includes a subsurface geotechnical exploration, a condition assessment report, and topographic surveys. Data from these sources provides both useful background information and quantitative inputs to the sediment model in this study.

A subsurface geotechnical exploration was performed by S&ME, Inc. on October 10, 2011. Eight perimeter soil borings were drilled, and a report was prepared to provide recommendations for foundation design in anticipation of a pond reconstruction project. To date, no such construction has occurred. The geotechnical report indicates bedrock at depths of 6 - 10 feet. One boring, B-4, indicates the presence of alluvium. All other borings indicate some degree of man-placed soils, or fill.

A Supplemental Stormwater Management Report, dated November 17, 2011, was prepared by Draper Aden Associates to characterize the duck pond condition and to provide recommendations for improvement. As part of this study, topographic surveys were performed around the perimeter of the duck pond to collect information on the pond geometry and surrounding topography.

In September, 2012, a pond inventory was performed to characterize the pond hydraulics, identify deficiencies, and provide specific input data for this study. A topographic survey and site investigation were performed and ultimately used to obtain the sediment volume accumulated between October 2011 and September 2012 (Section 3.4). Assuming the saturated sediment had a 50% porosity, it was estimated 170 tons of sediment accumulated in the pond during this time period. More detailed information on this calculation can be found in Section 3.4.1.

Chapter 2. Methodology

The Revised Universal Soil Loss Equation (RUSLE; Renard et al., 1997) was used to identify erosion hotspots and to estimate gross sediment erosion across the watershed. The Sediment Delivery Distributed (SEDD; Ferro & Porto, 2000) model was then used to determine sediment yield at the pond. The RUSLE and SEDD models were integrated with a raster GIS software package (ArcGIS), which allowed characterization of the watershed spatial heterogeneity (He and Walling, 2003). Figure 4 outlines the RUSLE and SEDD modeling processes. The RUSLE model is summarized in light blue across the top of Figure 4 and the SEDD model is summarized in light green in the bottom left of Figure 4.

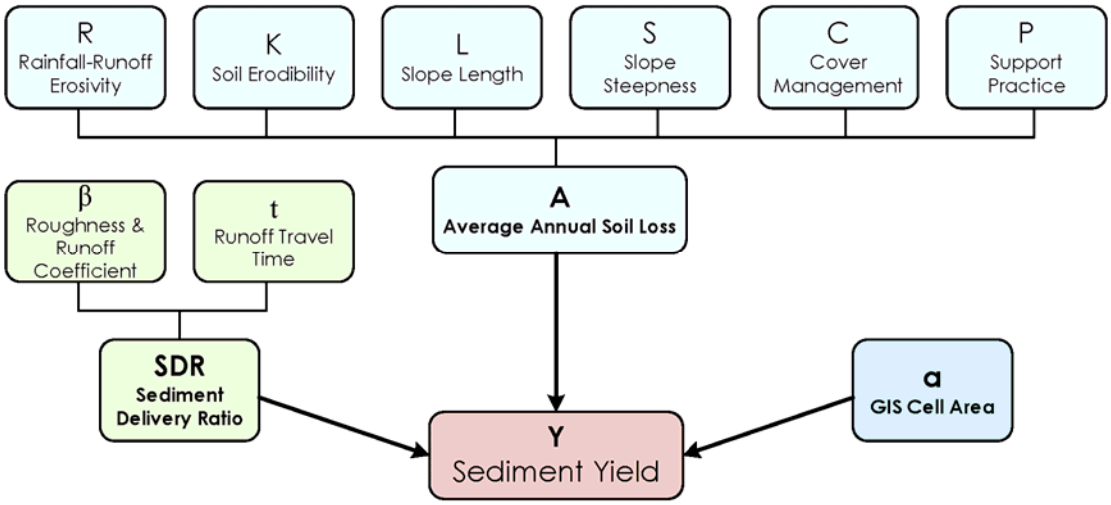

Figure 4. Sediment yield calculation flow chart

2.1. Gross Sediment Estimation - RUSLE

The Universal Soil Loss Equation was developed by the US Department of Agriculture (USDA), the Agricultural Research Service (ARS), the Soil Conservation Service (SCS), and Purdue University to predict average sheet and rill erosion from agricultural lands

(Wischmeier and Smith, 1978). Since its initial development, this empirical model has been modified to expand its capabilities, first as the Modified Universal Soil Loss Equation (MUSLE), and most recently as the Revised Universal Soil Loss Equation (RUSLE) (Renard et al., 1997). The RUSLE model is the most commonly used erosion prediction model to date. However, the model has limitations, including the inability to estimate deposition and gully, streambank, and streambed erosion.

The Water Erosion Prediction Project, or WEPP model, is an alternative erosion estimation model predicted to replace RUSLE in the future (Renard et al., 1997). WEPP is intended to take advantage of modern computing capabilities and have a broader range of applicability, but it is not yet fully vetted and requires additional development (Tiwari et al., 2000).

Because of its maturity and widespread accepted use, the RUSLE model was chosen for this project. The RUSLE model was originally developed for a single plot of land, but in recent decades, as computing and software capabilities have grown, it has been extended to watersheds (Tiwari et al., 2000). More specifically, GIS software has been used to perform RUSLE calculations using a raster grid of discrete morphological units, which are similar in scale to the original single plot application.

The RUSLE equation predicts the average annual soil loss A_i for each cell in the raster grid as follows. All terms in Equation 1 are uniquely defined for each cell in the grid except for the erosivity factor R, which is taken as a constant value for the entire watershed.

$$A_i = R \cdot K_i \cdot L_i \cdot S_i \cdot C_i \cdot P_i \qquad [1]$$

where:

A_i = average annual soil loss, $t \cdot (ac \cdot yr)^{-1}$
R = rainfall-runoff erosivity factor, $ft \cdot tonf \cdot in \cdot (ac \cdot h \cdot yr)^{-1}$
K_i = soil erodibility factor, $t \cdot ac \cdot h \cdot (ac \cdot ft \cdot tonf \cdot in)^{-1}$
L_i = slope length factor, dimensionless
S_i = slope steepness factor, dimensionless
C_i = cover and management factor, dimensionless
P_i = conservation practice factor, dimensionless

2.2. Sediment Delivery and Yield Estimation - SEDD

The Sediment Distributed Delivery (SEDD) model was selected to estimate sediment yield at the duck pond because of its consideration of spatial distribution and applicability to watersheds (Ferro and Porto, 2000). The SEDD model is empirical, based on the USLE, and includes a sediment delivery ratio (SDR) determined for each morphological unit in the watershed. The SEDD model was calibrated using rainfall, runoff, and sediment concentration data collected for three basins near Crotone, Italy. At the outfall of each basin, "water discharge, suspended sediment concentration, and rainfall were measured" using an H-flume, mechanical recording water level gauge, and a recording rain gauge (Ferro & Porto, 2000). To obtain the sediment yield, mean suspended sediment concentrations were determined from samples taken at various flow depths and then multiplied by the measured runoff volume (Ferro & Porto, 2000).

To estimate sediment yield for the relatively small duck pond watershed (1,194 acres), the SEDD model was adapted according to Fernandez et al., 2003. Using ArcGIS, yield calculations were performed for each grid cell and then summed across the watershed using the following equations (Ferro & Porto, 2000):

$$Y_i = SDR_i \cdot A_i \cdot a_i \quad [2]$$

$$Y = \sum_{i=0}^{N} Y_i \quad [3]$$

where:

Y_i = sediment yield for cell i, $t \cdot (yr)^{-1}$
SDR_i = sediment delivery ratio for cell i, dimensionless
A_i = average annual soil loss for cell i, $t \cdot (ac \cdot yr)^{-1}$
a_i = area of cell i, ac
Y = total sediment yield, $t \cdot (yr)^{-1}$

The SDR value describes the fraction of eroded sediment actually delivered to the point in question. It is reliant on flow and land characteristics by:

$$SDR_i = \exp(-\beta \cdot t_i) \quad [4]$$

where:

t_i = travel time from i^{th} cell to nearest stream reach, hr
β_i = roughness and runoff coefficient for cell i, dimensionless

The roughness and runoff coefficient (β) is defined by the watershed characteristics and was approximated using results from Ferro and Porto, 2000. β determination for this watershed is discussed in Section 3.2.1. The travel time t_i for a particular cell is the time it takes for runoff to travel from the i^{th} cell to the nearest stream reach along the morphological flow path and is found by summing the contributions of all of the cells along the flow path (Equation 5). In this expression, the segment path length l_i is equal to the length of either the side or diagonal of a cell depending on the flow direction in the cell (Fernandez et al., 2003). The runoff velocity (Equation 6) was estimated using the relationship presented in Haan et al., 1994:

$$t_i = \sum_{n=1}^{N} \frac{l_n}{v_n} \quad [5]$$

$$v_n = d_n S_n^{1/2} \quad [6]$$

where:

l_n = length of segment in flow path n, m
v_n = runoff velocity for cell n, m/s
d_n = surface roughness coefficient for cell n, m/s
S_n = slope for cell n, m/m

2.3. Data Sources

Publically available data from various sources was collected to implement the RUSLE and SEDD models in ArcGIS. A list of data sources is provided in Table 1. The precipitation data was used to calculate the rainfall-runoff erosivity factor. The aerial imagery was used to manually delineate the land cover categories and to determine surface characteristics, such as the surface roughness coefficient (SEDD model) and the C and P factors (RUSLE). The Soil Survey of Washington County Area and the City of Bristol contained already-calculated soil erodibility factors for each soil unit. The watershed was delineated manually using the topographic base mapping information. The topographic mapping was also used to create the digital elevation model in ArcGIS, which served as input for many of the RUSLE and SEDD calculations including the L and S factors (RUSLE).

Table 1. Model data sources

Data Description	Source
Precipitation	National Atmospheric & Oceanic Administration (NOAA)
Aerial Imagery	2007 Virginia Geographic Information Network (VGIN)
Soil Survey	USDA Natural Resources Conservation Service (NRCS)
Topography	2007 Virginia Base Mapping Program (VBMP)

Chapter 3. Results

3.1. RUSLE

The RUSLE model was applied to the 1,194 acre watershed by discretizing it into 100 foot by 100 foot morphological units, or grid cells, and calculating the RUSLE factors for each cell. ArcGIS zonal statistics were then used to calculate averages and sums to report results for each factor. This method used publically available rainfall data, aerial photography, topographic mapping, and soil survey information as described below as well as in Section 2.3.

3.1.1. Rainfall-Runoff Erosivity Factor - R

The rainfall-runoff erosivity factor was calculated using two methods. First, R was calculated using National Oceanic and Atmospheric Administration (NOAA) precipitation gauging data. The Troutdale 3 SSE station, located 22 miles southeast of the pond, was selected due to its proximity to the watershed and the availability of 15 minute precipitation data. R was calculated by (Renard et al., 1997):

$$R = \frac{\sum_{i=1}^{l}(EI_{30})_i}{N} \quad [7]$$

where:

R = rainfall erosivity factor, hundreds ft·tonf·in·(ac·hr·yr)$^{-1}$
N = number of years in the period, yr
l = number of storms in the period, dimensionless
I_{30} = maximum 30-minute rainfall intensity per storm, in·(hr)$^{-1}$
E = total rainfall energy per storm, ft·tonf·(ac)$^{-1}$

The total rainfall energy (E) is a function of the energy per unit of rainfall and the rainfall accumulation over the storm interval can be determined by (Renard et al., 1997):

$$E = \sum_{j=1}^{m} e_j \, \Delta V_j \quad [8]$$

$$e_j = 0.29\left[1 - 0.72e^{-0.05i}\right] \quad [9]$$

where:

e_j = energy per unit of rainfall, ft·tonf·(ac·in)$^{-1}$
i = rainfall intensity over a given rainfall interval j, in·(hr)$^{-1}$
ΔV_j = rainfall accumulation during jth interval, in
m = number of rainfall intervals

The analyzed accumulation period spans 347 days between October 2011 and September 2012. During that time period, precipitation records for the months of August, September, and October were incomplete. As a substitute, average R values from August-October, 2006 - 2010 were calculated, averaged, and added to R values calculated for the other nine months. An R value of 161 hundreds ft·tonf·in(ac·hr·yr)$^{-1}$ was calculated using this method.

The second method used to estimate R was interpolation from the isoerodent map of the eastern United States contained in the USDA Agricultural Handbook Number 703 (Renard et al., 1997). The R value estimated from the isoerodent map was 138 hundreds ft·tonf·in(ac·hr·yr)$^{-1}$. The isoerodent map is provided in Figure 5.

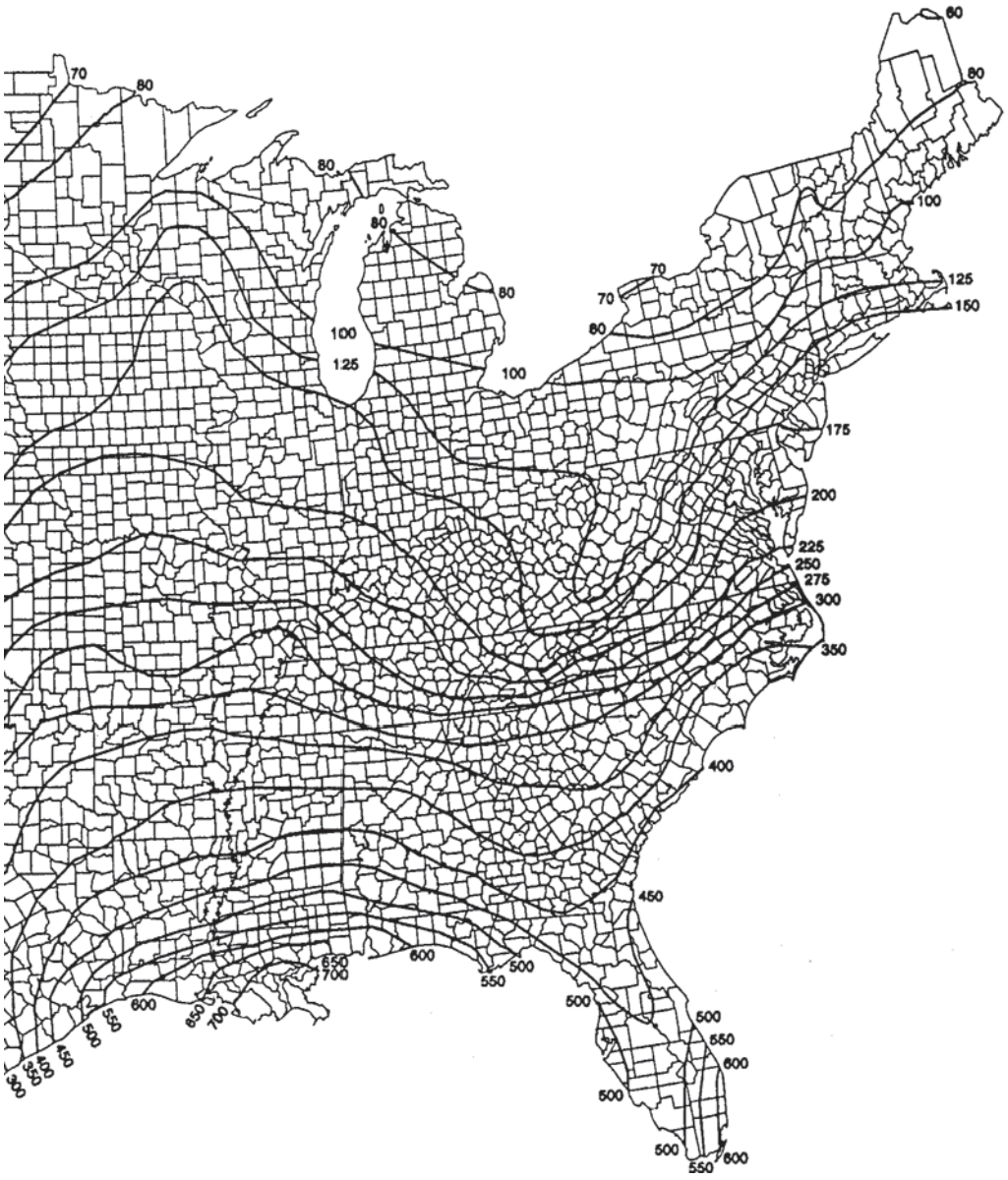

Figure 5. Isoerodent map of the eastern U.S. [Renard et al., 1997]

The calculated R value was 16% higher than the value taken from the isoerodent map. The values contained in the isoerodent map were calculated from the 22-year average of annual R values (Renard et al, 1997). Wischmeier, 1976, found that the storm erosivity (EI) for a specific rainfall event could range from less than half to more than double the 22-year average, which leads to variation in R values. Table 2compares the total accumulation value over the study period to the 5-yr, 10-yr, 20-yr, 50-yr, and

100-yr averages of annual precipitation. The data shows that the rainfall accumulated between October 2011 and September 2012 was between 6% and 11% higher than the long term rainfall averages, which is consistent with the larger calculated R value vs. the long term isoerodent map. The percent difference is lower for the more recent averages (5-, 10-, and 20-yr) because there is an observed increasing trend of 1.64 inches per century in the long term accumulation average.

Table 2. NOAA National Climatic Data - Virginia Climate Division 6

Duck Pond Accumulation Period	Rainfall (in)
Oct 2011 - Sep 2012	48.08

Avg of Annual Rainfall	Rainfall (in)	% Difference
5 year avg.	45.52	+ 6%
10 year avg.	45.21	+ 6%
20 year avg.	44.06	+ 9%
50 year avg.	43.47	+ 11%
100 year avg.	43.27	+ 11%

3.1.2. Soil Erodibility Factor - K_f

The soil erodibility factor for each soil unit was taken from the Soil Survey of Washington County Area and the City of Bristol, Virginia prepared by the USDA NRCS. The fine earth fraction (K_f), which is unadjusted for surface rock fragments, was selected for use in the RUSLE equation. K_f values by soil unit are listed in Table 3, and Figure 6 shows the spatial distribution of K_f values.

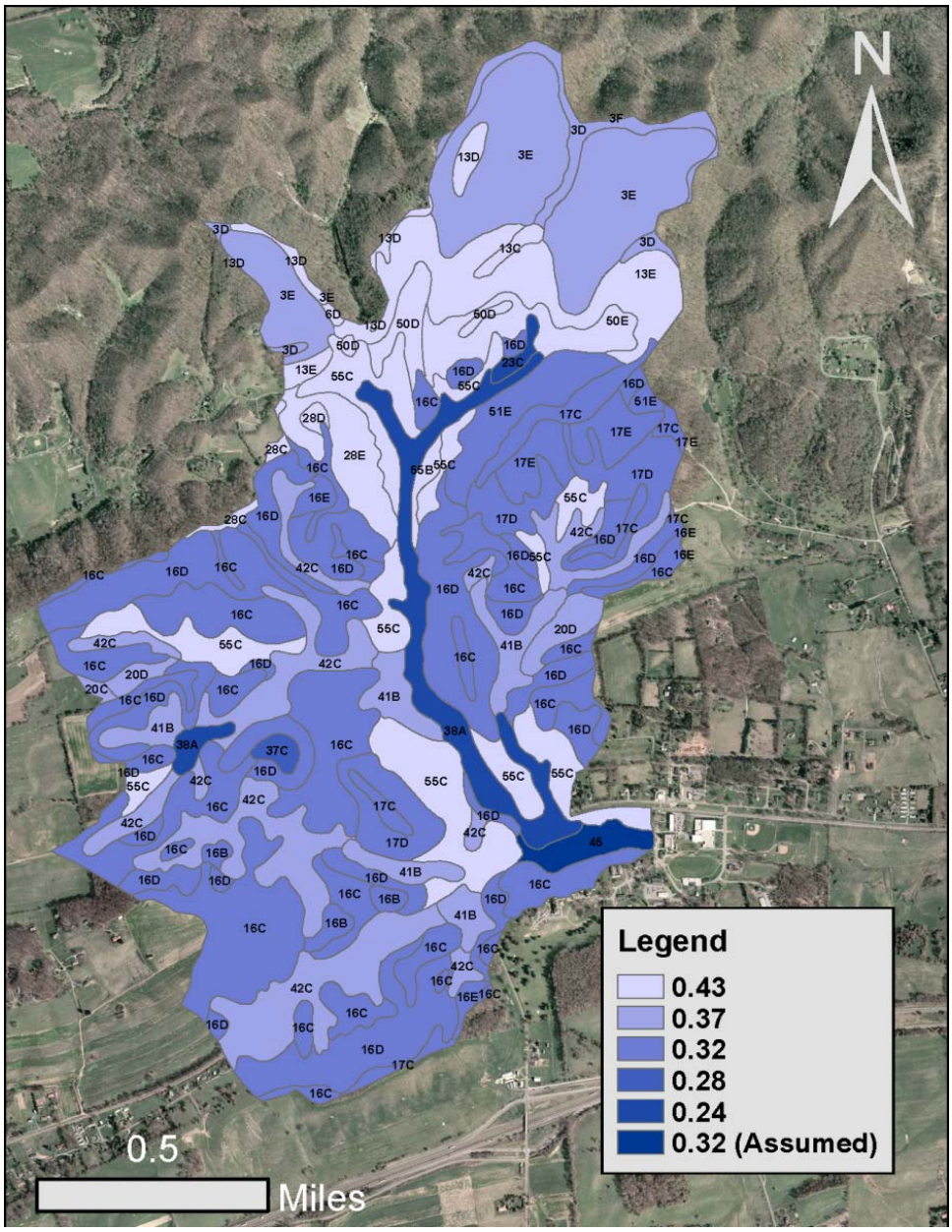

Figure 6. Map of by NRCS soil units and K_f values [t·ac·h(ac·ft·tonf·in)$^{-1}$] - [Data sources listed in Section 2.3]

Table 3. NRCS Soil Survey Data - Washington County, VA; K_f values in [t•ac•h(ac•ft•tonf•in)$^{-1}$]

Soil	Description	K_f
3D	Berks silt loam, 7 to 25 percent slopes	0.37
3E	Berks silt loam, 25 to 50 percent slopes	0.37
3F	Berks silt loam, 50 to 80 percent slopes	0.37
6D	Calvin silt loam, 7 to 25 percent slopes	0.43
13C	Elliber very gravelly silt loam, 7 to 15 percent slopes	0.43
13D	Elliber very gravelly silt loam, 15 to 25 percent slopes	0.43
13E	Elliber very gravelly silt loam, 25 to 65 percent slopes	0.43
16B	Frederick silt loam, 2 to 7 percent slopes	0.32
16C	Frederick silt loam, 7 to 15 percent slopes	0.32
16D	Frederick silt loam, 15 to 25 percent slopes	0.32
16E	Frederick silt loam, 25 to 45 percent slopes	0.32
17C	Frederick very gravelly silt loam, 7 to 15 percent slopes	0.32
17D	Frederick very gravelly silt loam, 15 to 25 percent slopes	0.32
17E	Frederick very gravelly silt loam, 25 to 45 percent slopes	0.32
20C	Hagerstown silt loam, 7 to 15 percent slopes, very rocky	0.37
20D	Hagerstown silt loam, 15 to 25 percent slopes, very rocky	0.37
23C	Hayter loam, 7 to 15 percent slopes	0.24
28C	Litz-Groseclose complex, 7 to 15 percent slopes	0.43
28D	Litz-Groseclose complex, 15 to 25 percent slopes	0.43
28E	Litz-Groseclose complex, 25 to 75 percent slopes	0.43
37C	Shottower loam, 7 to 15 percent slopes	0.28
38A	Sindion silt loam, 0 to 3 percent slopes, occasionally flooded	0.24
41B	Timberville-Marbie complex, 2 to 7 percent slopes, frequently flooded	0.37
42C	Timberville-Marbie complex, 7 to 15 percent slopes, rarely flooded	0.37
45	Udorthents, 0 to 25 percent slopes	0.32
50D	Weikert silt loam, 15 to 25 percent slopes	0.43
50E	Weikert silt loam, 25 to 50 percent slopes	0.43
51E	Westmoreland silt loam, 25 to 50 percent slopes, rocky	0.32
55B	Wyrick-Marbie complex, 2 to 7 percent slopes	0.43
55C	Wyrick-Marbie complex, 7 to 15 percent slopes	0.43

Soil unit 45, Udorthents, is an urban land complex that describes soils affected by manmade land disturbance and development activities such as excavation, fill, and compaction (USDA 1993). This unit was only found on the EHC campus. K_f values for this soil unit are not provided in the Soil Survey; therefore, a value was assumed for soil unit 45. The higher the K_f value, the more susceptible the soil is to erosion.

With this in mind, it is expected that the urban land complex would experience higher than average erosion due to land disturbance activities, but this might be balanced by increased amounts of stabilizing impervious cover. Because of this, the median Kf value of 0.32 was selected.

3.1.3. Slope Length Factor - L

The slope length factor accounts for the influence of topography on soil erosion and "is defined as the horizontal distance from the origin of overland flow to the point where either (1) the slope gradient decreases enough that deposition begins or (2) runoff becomes concentrated in a defined channel" (Wischmeier & Smith, 1978). In these terms, L is defined as (Al-Smadi, 2007):

$$L_{i,j} = \frac{\lambda_{i,j}^{m+1} - \lambda_{(i,j)-1}^{m+1}}{\left(\lambda_{i,j} - \lambda_{(i,j)-1}\right)22.13^{m}} \quad [10]$$

Where:

$L_{i,j}$ = slope length factor for grid cell with coordinates (i,j), m
$\lambda_{i,j}$ = length from top of slope to lower end of $(i.j)^{th}$ grid cell, m
$\lambda_{(i,j)-1}$ = length from top of slope to upper end of $(i,j)^{th}$ grid cell, m
m = slope length exponent (defined below)

For application in raster GIS, the slope length factor can be considered in terms of the upstream contributing drainage area to each discrete cell in the watershed (Desmet and Grovers, 1996; Fernandez et al., 2003).

$$L_{i,j} = \frac{U_{i,j-out}^{m+1} - U_{i,j-in}^{m+1}}{\left(U_{i,j-out} - U_{i,j-in}\right)22.13^{m}} \quad [11]$$

The term $U_{i,j}$ denotes the contributing area per contour width and is used as a means of converting the length-based calculation to an area-based calculation, which is more easily implemented in ArcGIS. A length slope limit of 400 ft, or a maximum of four contributing grid cells, was established using the ArcGIS flow accumulation tool (Renard et al., 1997). Figure 7 demonstrates the effect the flow accumulation limit had on the L factor. L factor values were limited to a range of 1 - 6.3. The area-based flow accumulation formula is defined as (Fernandez et al., 2003):

$$U_{i,j-in} = (\#\ of\ cells\ feeding\ cell\ i,j) \cdot \frac{cell\ area}{cell\ length} \quad [12]$$

$$U_{i,j-out} = cell\ length + U_{i,j-in} \quad [13]$$

The units of area and length are in meters squared and meters to agree with the constant value 22.13 in Equation 11. The value of the slope length exponent m is calculated from the ratio of rill to interrill erosion (ρ). This ratio is determined from the topographic slope angle θ (in radians) as follows (Renard et al., 1997):

$$m = \frac{\rho}{(1+\rho)} \quad [14]$$

$$\rho = \frac{\frac{sin\theta}{0.0896}}{3(sin\theta)^{0.8} + 0.56} \quad [15]$$

Calculated values of L and ρ are shown in Figure 7. Generally, both the L value and the ρ ratio follow closely the slope of each cell. In the steeper regions of the graph, the model predicts over 2x more rill erosion than interrill. In the low-lying areas, this ratio is inverted, and the model accounts for almost 100% of the erosion as being

interrill. The map of L appears significantly more complex than ρ, which is a result of the fine features in the raster flow direction field.

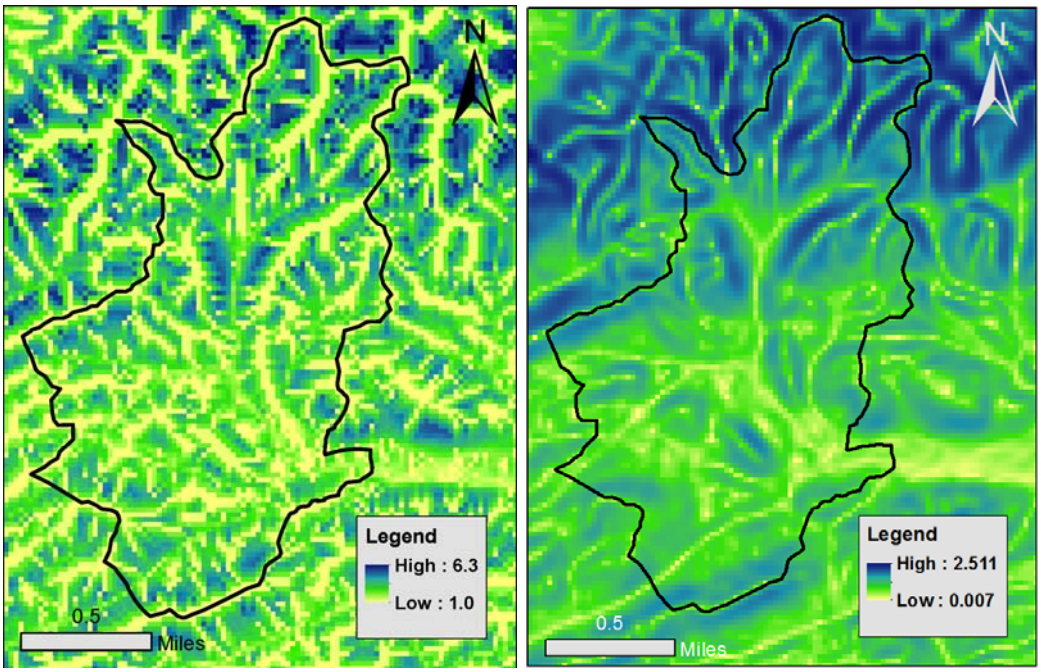

Figure 7. Raster map of: (left) slope length factor L, and (right) ratio of rill to interrill erosion ρ

3.1.4. Slope Steepness Factor - S

Soil erosion increases with slope steepness. The slope steepness factor S describes this phenomenon and is broken down into two categories as follows (Renard et al., 1997):

$$S = 10.8 sin\theta_i + 0.03; \quad \theta_i < 5.14° \qquad [16]$$

$$S = 16.8 sin\theta_i - 0.50; \quad \theta_i \geq 5.14° \qquad [17]$$

where:

θ_i = slope angle for cell i, degrees

5.14° = reference steepness slope (9%)

Calculated values for S are shown in Figure 8. As expected, areas with steeper slopes had larger S values, which are shown in dark blue in Figure 8. Many references

combine the discussion of slope length factor L and steepness factor S into a single term, LS. According to the RUSLE Handbook Number 703, the combined LS factor represents the ratio of soil loss on a given slope length and steepness to soil loss from a reference plot with a slope length of 72.6 ft and a steepness of 9%,. Table 4 lists the calculated LS values, averaged by land use category, which match well with the values in Tables 4.1-4.3 in Renard et al., 1997. As shown in Table 4, the forested land category exhibited the steepest average land slope and the largest average LS value. Conversely, the urban and cropland categories had the flattest average land slopes and the smallest average LS values.

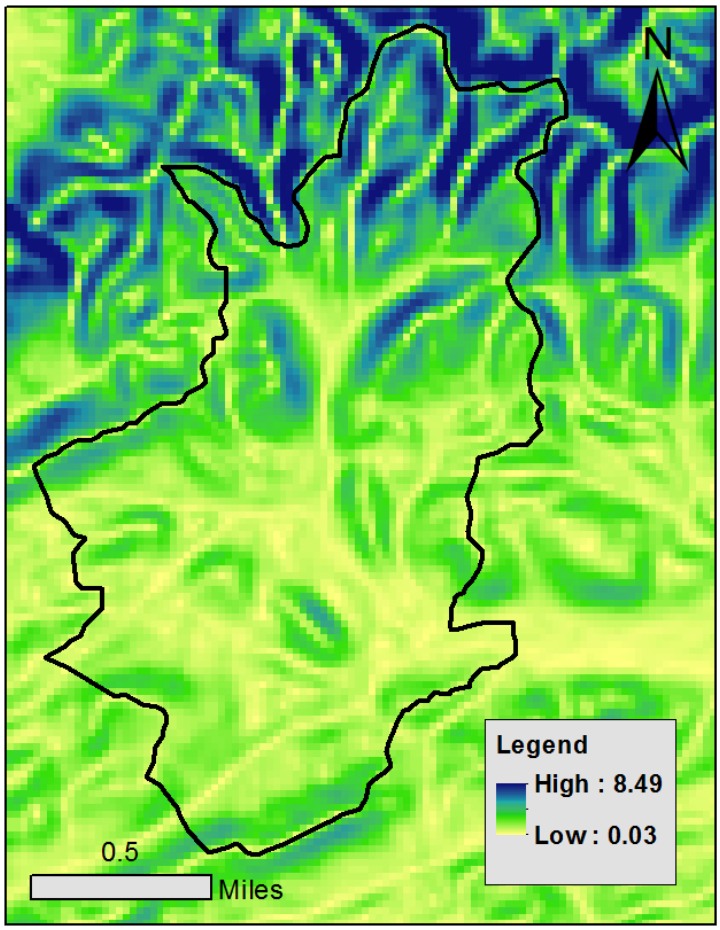

Figure 8. Raster map of slope steepness factor S

Table 4. Calculation of slope length and steepness factors, averaged by land use category

Land Use	Area (ac)	Slope (%)	ρ	m	L	S	LS
Forested	372	20.7	1.56	0.60	2.88	2.97	9.10
Grassland	282	9.4	0.97	0.47	2.38	1.19	3.12
Urban	305	8.6	0.91	0.46	2.39	1.07	2.84
Cropland	172	8.7	0.94	0.47	2.44	1.06	2.79
Harvested Forest	64	17.9	1.48	0.59	2.69	2.52	7.09

3.1.5. Cover Management Factor - C

The RUSLE cover management factor C is a function of land management practices, or the lack thereof, and how they affect soil erosion rates. The C factor is dependent on the soil loss ratio SLR and the storm erosivity EI as follows (Renard et al., 1997):

$$C = \frac{\sum_{i=1}^{n}(SLR_i \cdot EI_i)}{EI_i} \quad [18]$$

The soil loss ratio SLR is comprised of six factors as follows:

$$SLR_i = PLU_i \cdot CC_i \cdot SC_i \cdot SR_i \cdot SM_i \quad [19]$$

where:

PLU = prior land use factor
CC = canopy cover factor
SC = surface cover factor
SR = surface roughness factor
SM = soil moisture factor

Exact cover and management information was unknown for every parcel in the watershed. Each subarea was manually delineated using ArcGIS and identified using aerial imagery and information from the Virginia Cooperative Extension Agent (Extension Agent) for Washington County (Blevins). C values for similar land cover categories were used from the literature to estimate a C value for each of the 40 sub

areas (Wischmeier & Smith, 1978; Dissmeyer & Foster, 1980, Haan et al, 1994). Assigned values for C are shown in Figure 9.

According to the USDA 2007 Census of Agriculture, forage crops, corn, and tobacco are the top three field crops grown in Washington County, Virginia (www.agcensus.usda.gov). The Extension Agent helped to identify the cropping systems grown on the agricultural areas, which were determined to be corn, grass hay/pasture, and corn followed by a small grain cover crop. Then, for each subarea, a weighted C value was calculated to reflect contributions from each cover category.

From USDA Handbook Number 537, C values for harvested forest were estimated from Tables 11 and 12, and C values for grass hay/pasture were estimated from Table 10. C values for corn were estimated from Table 8.9 in Haan et al. 1994. All C values were then compared to those published in Fernandez et al. 2003, Haan et al., 1994 and Dissmeyer & Foster, 1980 with good agreement.

Higher C values, shown in dark blues/greens in Figure 9, correspond to cover management conditions that contribute more erosive potential than the lower C values, shown in light green and yellow. For example, the harvested forest located in the northeastern part of the watershed (shown in blue) has a C value of 0.2, whereas the stable forest immediately to the north, east, and west of the harvested forest (shown in yellow), has a C value of 0.001. Table 5 lists the average C values for each land cover category.

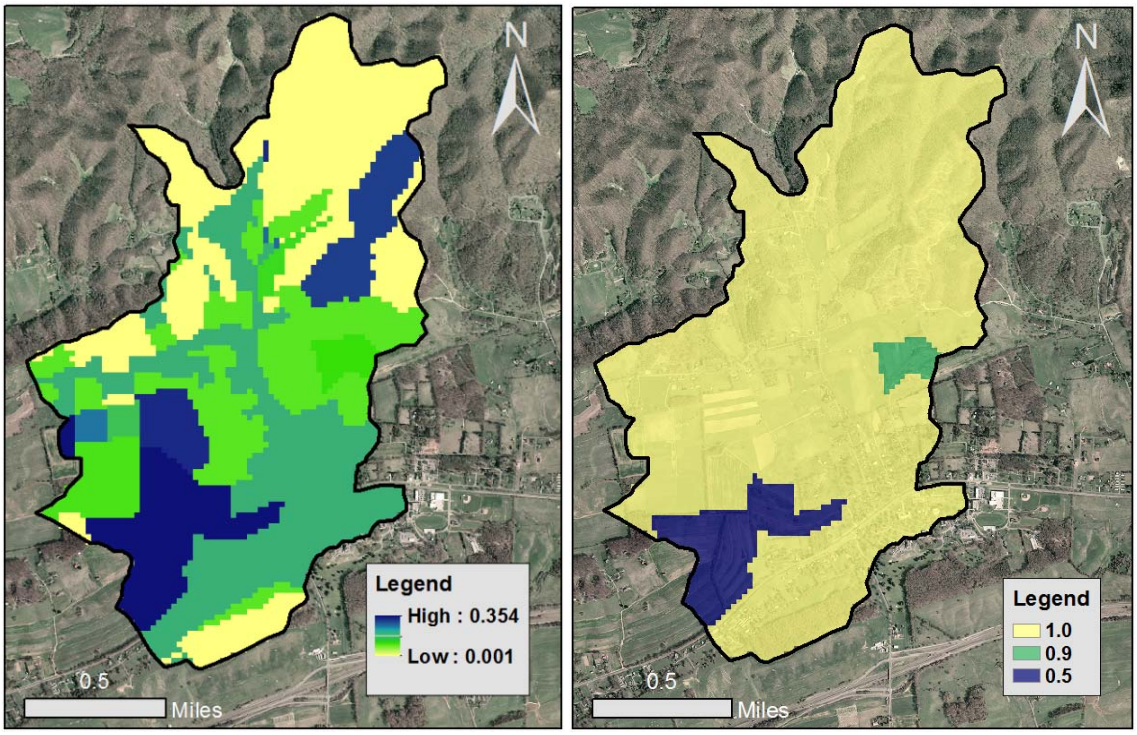

Figure 9. Raster map of: (left) cover management factor C, and (right) support practice factor P [Data sources listed in Section 2.3]

3.1.6. Support Practice Factor - P

The support practice factor P accounts for land modification practices that may reduce the amount and rate of runoff (Renard and Foster, 1983). Land disturbance associated with farming activities increase infiltration and reduces runoff, which can then be paired with support practices such as contour furrowing, ripping, grubbing, and root plowing to further control runoff and promote sedimentation (Renard et al., 1997).

All subareas with the exception of two areas were assigned a support practice factor of 1, meaning that no practice was implemented to control erosion. From the aerial imagery and topography, it was determined that two subareas implemented varying degrees of contour farming. These areas have P factors of 0.5 and 0.9 and are shown

in blue and green, respectively, in Figure 9. Contouring helps to reduce the velocity of runoff and promote sedimentation, hence the reason why the P factors for these two farms are smaller than those for the rest of the watershed. Support practice factors were estimated from Table 8.13 in Haan et al., 1994.

3.1.7. Average Annual Soil Loss - A

Using raster calculation tools in ArcGIS, the average annual soil loss A_i was determined for each discrete cell in the watershed. Calculated values for A_i are shown in Figure 10 and summarized in Table 5. As expected, the harvested forest and croplands experienced the most erosion and the stable forested areas the least. The urban areas account for 26% of the drainage area but only contribute 11.7% to the average annual soil loss. Similarly, the forest and grasslands account for 31% and 24% of the drainage area, respectively, but only contribute 1.6% and 4.4% to the average annual soil loss. Conversely, the harvested forest and croplands account for 5% and 14 % of the total drainage area, respectively, but contribute 42.1% and 40.3% to the average annual soil loss.

When compared across similar land-use categories, the calculated soil loss A_i in this study was between 3 and 4 times the amount calculated by Fernandez et al., 2003. Further comparison of the RUSLE factors is provided in Section 4.3.

Although these factors are significantly different, it is realistic to expect that the watershed erosivity and slope-derived terms should be higher in the mountains of Southwestern Virginia than they would be in the region of Western Idaho studied by Fernandez, et al., 2003.

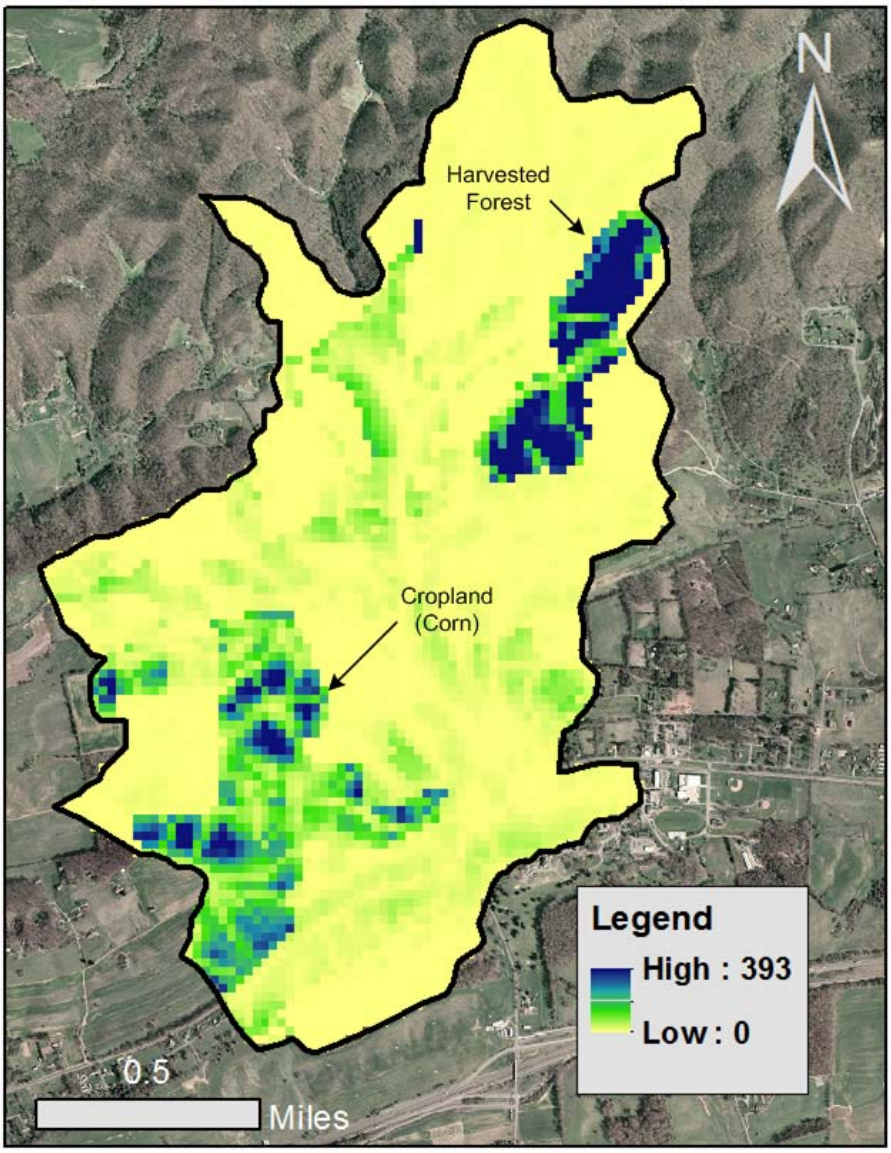

Figure 10. Raster map of average annual soil loss A [t·(ac·yr)$^{-1}$] - [Data sources listed in Section 2.3]

3.2. SEDD

The Sediment Delivery Distributed Model was developed by Ferro and Porto, 2000 as a means to model sediment delivery processes at the basin scale. The model inputs gross eroded sediment from the RUSLE equation and determines the sediment yield, or how much of the eroded sediment is transported to a downstream location. The method involves the calculation of a sediment delivery ratio for each morphological unit or grid cell using raster GIS.

3.2.1. Sediment Delivery Ratio, SDR

The sediment delivery ratio concept has been presented by many researchers (Boyce, 1975; Ferro and Minacapilli, 1995). Generally, the SDR decreases as the watershed area increases because there are more opportunities for eroded sediment to settle or be re-captured by the watershed before reaching a stream (Boyce, 1975). Ferro and Porto define the sediment delivery ratio according to Equation 4, which contains a basin-specific parameter β.

The roughness and runoff coefficient β can be estimated using an inverse modeling approach, where the SDR for a watershed is related to β as a weighted mean of SDR_i (Fernandez et al., 2003). However, because the watersheds used by Ferro and Porto to calibrate the SEDD model were similar to the EHC duck pond watershed, most notably because both included harvested forests, a β value of 0.0186 was estimated from their results. A β sensitivity analysis is provided in 4.1.4.

The travel time t_i is the time it takes for runoff to flow from the i^{th} cell to the nearest stream reach along the morphological flow path. Ferro and Porto presented the following relationship for calculating the travel time along each morphological unit i:

$$t_{p,i} = \frac{l_{p,i}}{\sqrt{s_{p,i}}} = \sum_{j=1}^{N_p} \frac{\lambda_{i,j}}{\sqrt{s_{i,j}}} = \sum_{i=1}^{N_p} \frac{l_i}{v_i} \quad [20]$$

where:

$t_{p,i}$ = travel time for particles eroded from cell i, hr
$l_{p,i}$ = length of the hydraulic flow path, ft
$s_{p,i}$ = slope of hydraulic flow path, ft/ft
N_p = number of morphological units, dimensionless
j = hydraulic flow path, dimensionless
$\lambda_{i,j}$ = length of morphological unit, ft
$s_{i,j}$ = slope of morphological unit, ft/ft
l_i = length of segment i along the flow path, which is the length of the side or diagonal of a cell depending on the flow direction in the cell, ft
v_i = velocity for cell i, ft/s

Chezy's uniform open channel flow equation states that the $\sqrt{s_{i,j}}$ is proportional to the flow velocity v_i yielding the final relationship of $t_i = l_i/v_i$ (Ferro and Porto, 2000). The velocity equation for overland and shallow concentrated flow, Equation 6, presented by the SCS TR-55 manual was then used to determine velocity (SCS TR-55, 1975; Haan et al, 1994; Fernandez et al, 2003). The surface roughness d_i was taken from Table 3.20 in Haan et al, 1994. The velocity was calculated as follows:

Calculated values for travel time t_i along with the digital elevation model are shown in Figure 11 and calculated SDR values are shown in Figure 12. Generally, assuming everything else the same, the closer the morphological unit is to the duck pond, the higher the SDR value. As expected, very little sediment from the farthest points in the watershed is predicted to reach the duck pond, as indicated by low SDR values

and large travel times in the more distant areas. The model predicted that it takes 429 hours, or 17.9 days, for water to travel from the farthest reaches of the watershed to the duck pond.

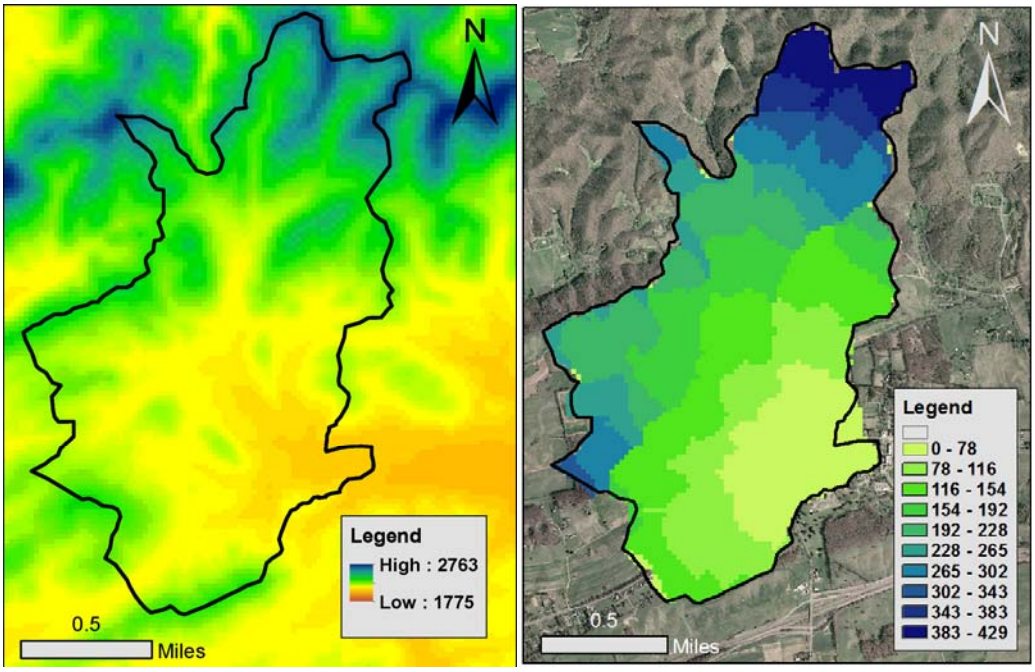

Figure 11. Raster map of: (left) digital elevation model and, (right) travel time, hr

[Data sources listed in Section 2.3]

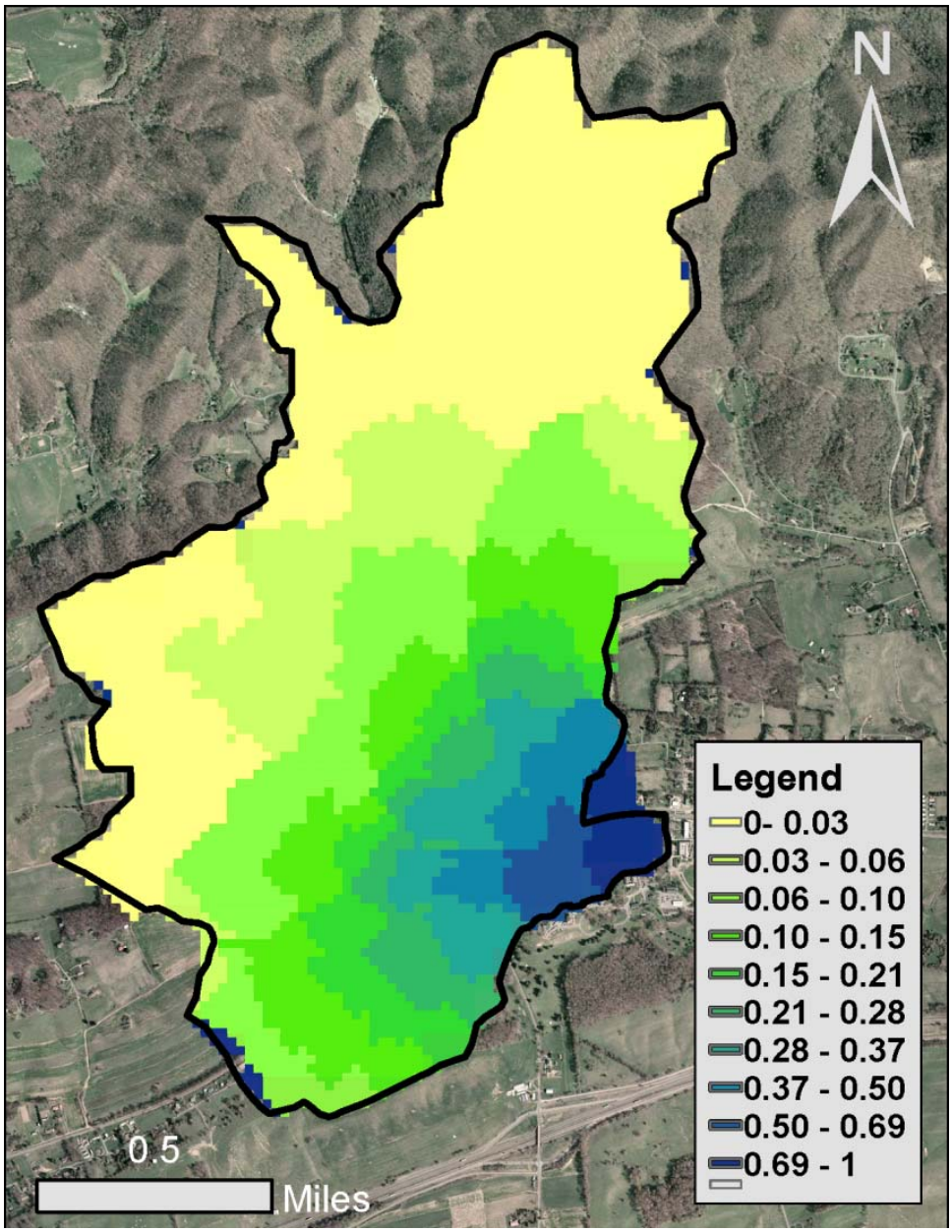

Figure 12. Raster map of sediment delivery ratio SDR [Data sources listed in Section 2.3]

3.2.2. Sediment Yield

Total sediment yield at the duck pond was calculated by summing individual yield values across the watershed according to Equation 3. For each morphological unit, or grid cell, the sediment yield was calculated using ArcGIS raster calculation tools using Equation 2.

Calculated values for Y_i are shown in Figure 13. Similar to the average annual soil loss pattern shown in Figure 10, the sediment yield values are highest for the harvested forest and cropland subareas. However, particularly in the case of the harvested forest sub-areas, the large annual soil loss in some regions is mitigated by their distance from the duck pond (and correspondingly low SDR value). More specifically, the two circles shown in Figure 13, Section A and Section B, together outline the approximate limits of the harvested forest. The sediment yield calculations revealed that even though the entire area experienced significant erosion (Figure 10), not all of the eroded sediment was predicted to reach the duck pond. Much less sediment from Section A was predicted to reach the pond compared to the amount from Section B. Section A accounts for 50 % of the harvested forest portion of the contributing drainage area. Likewise, Section B accounts for the other 50% of the harvested forest drainage area. The difference in SDR values, specifically the travel distances, explains why erosion from half of the harvested forest is predicted to reach the duck pond and why the other half is not.

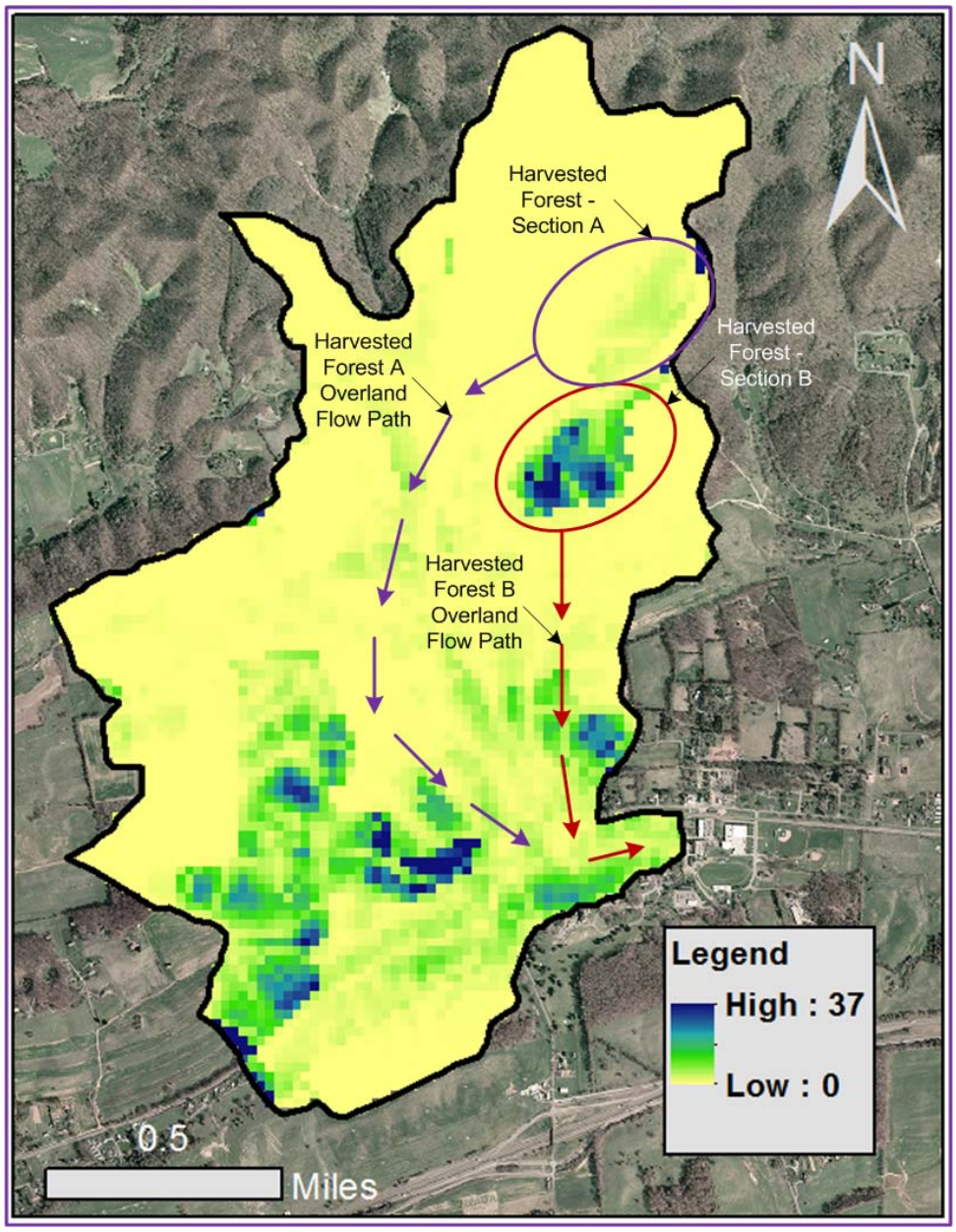

Figure 13. Raster map of sediment yield Y_i in $t(yr)^{-1}$ [Data sources listed in Section 2.3]

3.3. Combined Model Results

Modeled RUSLE and SEDD results are provided in Table 5 and Table 6.

Table 5. Summary of RUSLE model for Emory & Henry Duck Pond Watershed

Land Cover	Area	Area %Total	R	Kf	LS	C	P	A	A % Total
	ac		*	**	-	-	-	$t\cdot(ac\cdot yr)^{-1}$	
Forested	372	31%	161	0.37	9.1	0.001	1.0	0.5	1.6%
Grassland	282	24%	161	0.34	3.1	0.012	1.0	2.0	4.4%
Urban	305	26%	161	0.35	2.8	0.030	1.0	4.9	11.7%
Cropland	172	14%	161	0.34	2.8	0.293	0.7	29.9	40.3%
Harvested Forest	64	5%	161	0.36	7.1	0.200	1.0	84.6	42.1%

Table 6. Summary of SEDD model for Emory & Henry Duck Pond Watershed

Land Cover	Area	SDR	Y	Y * % Total
	ac	-	t·(ac·yr)-1	%
Forested	372	0.07	0.02	0.6%
Grassland	282	0.09	0.11	2.9%
Urban	305	0.26	0.97	27.5%
Cropland	172	0.11	2.93	46.9%
Harvested Forest	64	0.06	3.72	22.0%

It is interesting to note that the harvested forest accounts for 5% of the total watershed area and contributes 42.1% to the predicted average annual erosion. Due to the watershed characteristics, only 22% of the total sediment yield comes from this land category. Runoff from the harvested forest concentrates in two main areas. The first area has a more direct path to the duck pond with steeper slopes. The second area has a more circuitous path with flatter slopes as shown in Figure 13. Even though a considerable amount of sediment originates from the total harvested area, the amount delivered to the duck pond varies and is greatly dependent on the flow path distance and slope.

The cropland only accounts for 14% of the total watershed area, but contributes 40.3% to the average annual erosion and to almost half of the sediment yield. This is because of the cropland's erodibility and location in the watershed. The cropland is generally close to areas with concentrated flow and is also close to the duck pond, which has a major influence on the sediment delivery ratio.

3.4. Sediment Accumulation Measurement

For comparison to the sediment yield model, the duck pond was surveyed to compute the actual amount of accumulated sediment over a known period of time (347 days).

3.4.1. Topographic Survey

While drained for repairs, the duck pond sediment accumulation was surveyed on September 11, 2012. Vertical and horizontal topographic information was collected at over 150 survey points to calculate the sediment volume and at over 350 additional points to characterize the pond geometry and surrounding topography. After control was established using a total station, information on the top and bottom of the sediment was collected using a survey rod with integrated GPS. At each survey point, the rod was positioned on the top surface careful not to let the rod sink into the sediment. The rod was then pressed as far down into the sediment as possible to collect information on the pond bottom, which, according to EHC staff, is solid bedrock.

Three-dimensional surfaces of the duck pond were created from the topographic survey data using AutoCAD Civil 3D and are shown in Figure 14 and Figure 15. The pond inlet stream is located to the west and the outlet structure is located to the east

(north is oriented to plan north). The Civil 3D model was then used to determine the volume of accumulated sediment by creating a differential volumetric surface. The top and bottom surfaces were inputted as boundaries. Civil 3D computed an unadjusted differential volume of 210 yd^3.

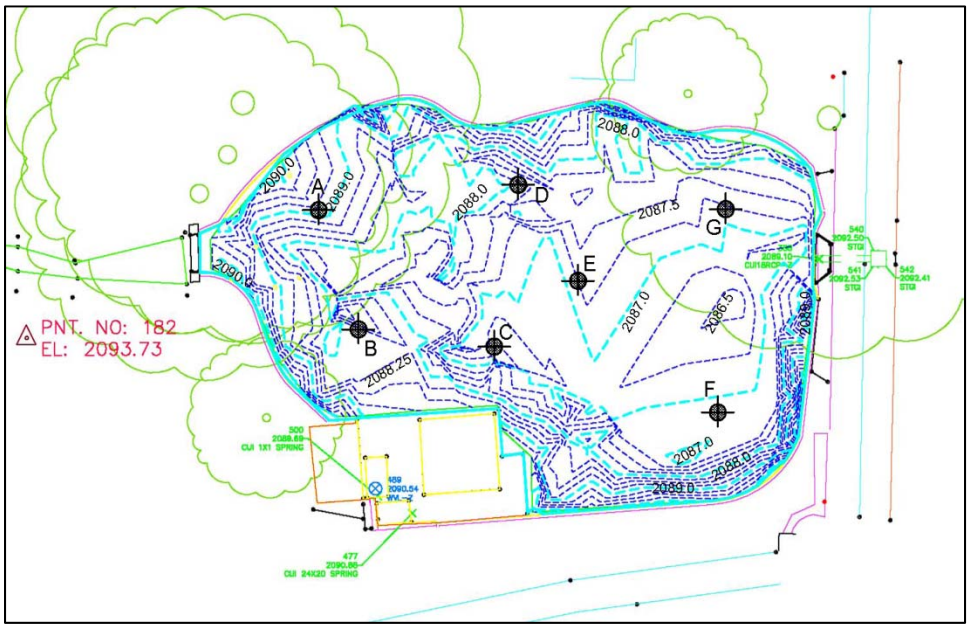

Figure 14. Duck pond topographic survey - sediment top surface, 0.25 ft contour interval with sediment sample locations A through G

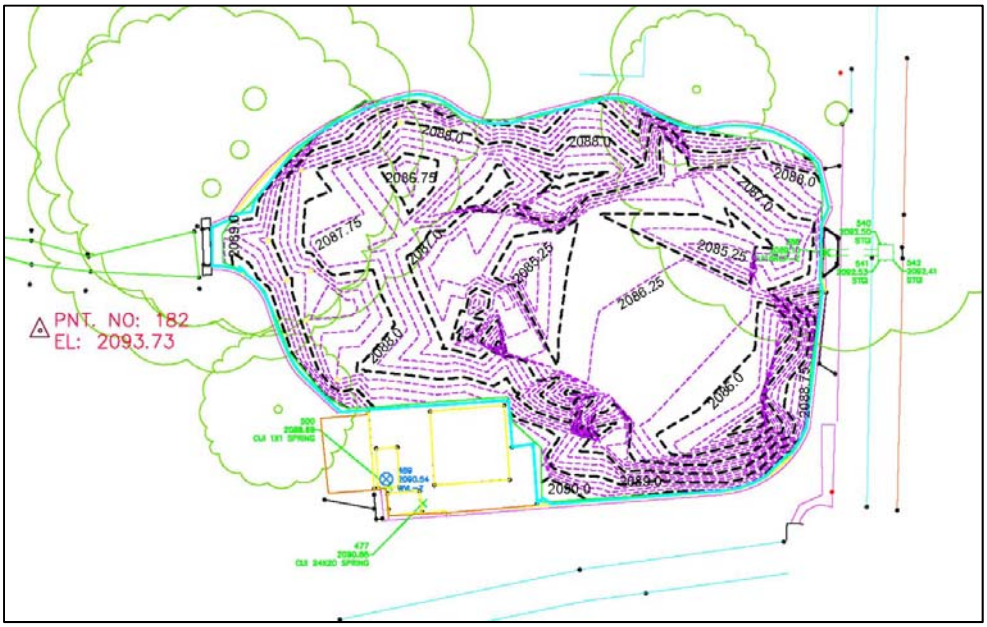

Figure 15. Duck pond topographic survey - sediment bottom surface, 0.25 ft contour interval

In the saturated pond environment, it was assumed that 50% of this volume was occupied by water (http://www.agriinfo.in). Geotechnical borings indicated the alluvium to be sandy silt, which was assumed to have a particle density of 120 $lb(ft)^{-3}$ (www.Stanford.edu). Based on this density, it was determined that 170 tons of sediment had accumulated in the pond between October 2011 and September 2012 (347 days).

3.4.2. Pond Residence Time vs. Sediment Settling Times

Because of the small pond size and observable short residence time, it was postulated that portions of the finer sediment do not have time to settle in the pond and might continue downstream. To test this hypothesis and interpret the sediment volume measurement, duck pond residence times were calculated for various flowrates and compared to calculated discrete particle settling times.

The theoretical pond residence time, or the average time a fluid particle remains in the pond, is the ratio of the total pond volume to the influent volumetric flow rate (Hossain et al., 2005). In reality, some fluid particles will short circuit the pond resulting in below average residence times, and others will be trapped in dead zones resulting in above average residence times. Because of the ephemeral nature of the inlet stream and the unknown quantity of contributing spring water, the theoretical residence time was calculated using the outlet flowrate.

The concrete pond outlet structure has a 20-inch diameter circular orifice approximately 4.6 feet above the pond bottom and a 1 foot by 5.8 foot rectangular

weir approximately 7.2 feet above the pond bottom. The following equations, adapted from Finnemore & Franzini, 2002, were used to calculate the outlet flowrate:

$$Q(weir) = C_{d-w}\,{}^{2}/_{3}\sqrt{2g}LH^{3/2} \quad [21]$$

$$C_{d-w} = 0.605 + \frac{1}{305H} + 0.08\frac{H}{P} = 0.62 \quad [22]$$

$$Q(co) = C_{d-co}\frac{\pi}{4}D^2\sqrt{2gh} \quad [23]$$

$$C_{d-co} = 0.86 \quad [24]$$

where:

Q(weir) =	Rectangular weir flowrate, $ft^3(s)^{-1}$
C_{d-w} =	Rectangular weir coefficient of discharge, dimensionless
g =	Acceleration due to gravity, 32.2 $ft(sec)^{-2}$
L =	Length of weir opening (5.8 ft), ft
H =	Water height above the crest (1 ft), ft
P =	Crest height (7.2 ft), ft
Q(co) =	Circular orifice flowrate, $ft^3(s)^{-1}$
D =	Circular orifice diameter, ft
h =	Difference in energy head between the upstream section and the minimum section of the circular opening (in this case h = D), ft
C_{d-co} =	Circular orifice coefficient of discharge (Figure 11.12, Finnemore & Franzini 2002), dimensionless

The College plugs the 20-inch circular orifice unless the rectangular weir cannot handle the peak flowrate, at which time the plug is removed and both outlets are used simultaneously. This flood control scheme is illustrated by Figure 16. For flowrates less than 19.3 cfs, the weir acts as the primary outlet. When the flowrate reaches 19.3 cfs, which corresponds to the maximum weir height, it is assumed that the 20-inch circular orifice plug is removed and both outlets operate simultaneously. The maximum combined outlet flow before the pond is breached is 33.4 cfs.

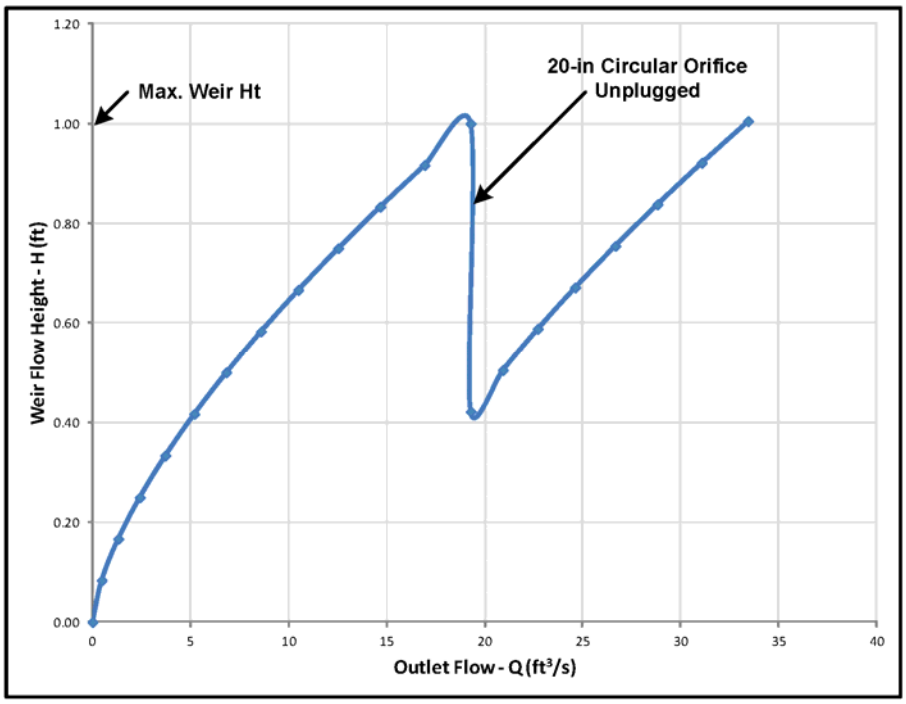

Figure 16. Weir flow height vs. outlet flowrate

Theoretical pond residence times were then calculated using the calculated flowrates and an approximated pond volume of 2,027 yd^3. The volume was estimated using information from the topographic survey. Pond volume approximation and sediment measurement limitations are discussed in Section 4.1.5. Theoretical residence times were calculated using a technique modified from Hossain et al., 2005 as follows:

$$RT_T = \frac{Total\ Pond\ Volume}{Volumetric\ Flowrate \cdot 3600} \quad [25]$$

where:

RT_T =	Theoretical residence time, hr
Total Pond Volume =	2,027 yd^3
Volumetric Flowrate =	Pond outlet flowrate, $ft^3(sec)^{-1}$

To account for dead zones and to reflect a more realistic pond efficiency, the theoretical residence times were adjusted using the following equation (Thackston et al., 1987):

$$\frac{\bar{t}}{T} = 0.84\left[1 - exp\left(-0.59\frac{L}{W}\right)\right] \quad [26]$$

where:

$\bar{t}$ = Adjusted residence time, hr

T = Theoretical residence time, hr

$\frac{L}{W}$ = Pond length to width ratio (1.57), dimensionless

Results for the theoretical and adjusted residence times are contained in Table 7.

Table 7. Theoretical and adjusted duck pond residence times

Total Pond Volume (yd^3)	Pond L/W Ratio
2,027	1.57

Outlet Flow (ft^3/s)	Theoretical Residence Time (hr)	Adjusted Residence Time (hr)
0.5	32.76	16.62
1.3	11.58	5.88
2.4	6.30	3.20
3.7	4.09	2.08
5.2	2.93	1.49
6.8	2.23	1.13
8.6	1.77	0.90
10.5	1.45	0.73
12.5	1.21	0.62
14.7	1.04	0.53
16.9	0.90	0.46
19.3	0.79	0.40
20.9	0.73	0.37
22.7	0.67	0.34
24.6	0.62	0.31
26.7	0.57	0.29
28.8	0.53	0.27
31.1	0.49	0.25
33.4	0.45	0.23

Seven (7) duck pond sediment samples were collected on May 7, 2013 to determine the particle size distribution of the accumulated sediment and to ultimately calculate the particle settling times. The samples were collected in a grid-like pattern in seven discrete locations as shown on Figure 14. Sample A was closest to the inlet stream, and Sample G was closest to the pond outlet structure. It was expected that larger diameter particles would be found in Sample location A near the pond inlet, but this was not the case. Unexpectedly, Samples A and G had the same sand composition. The grain size distribution was determined using sieve and hydrometer analysis according to ASTM D422-63: Standard Test Method for Particle-Size Analysis of Soils. Results for the measured sediment particle size distribution analysis are contained in Figure 17 and Table 8.

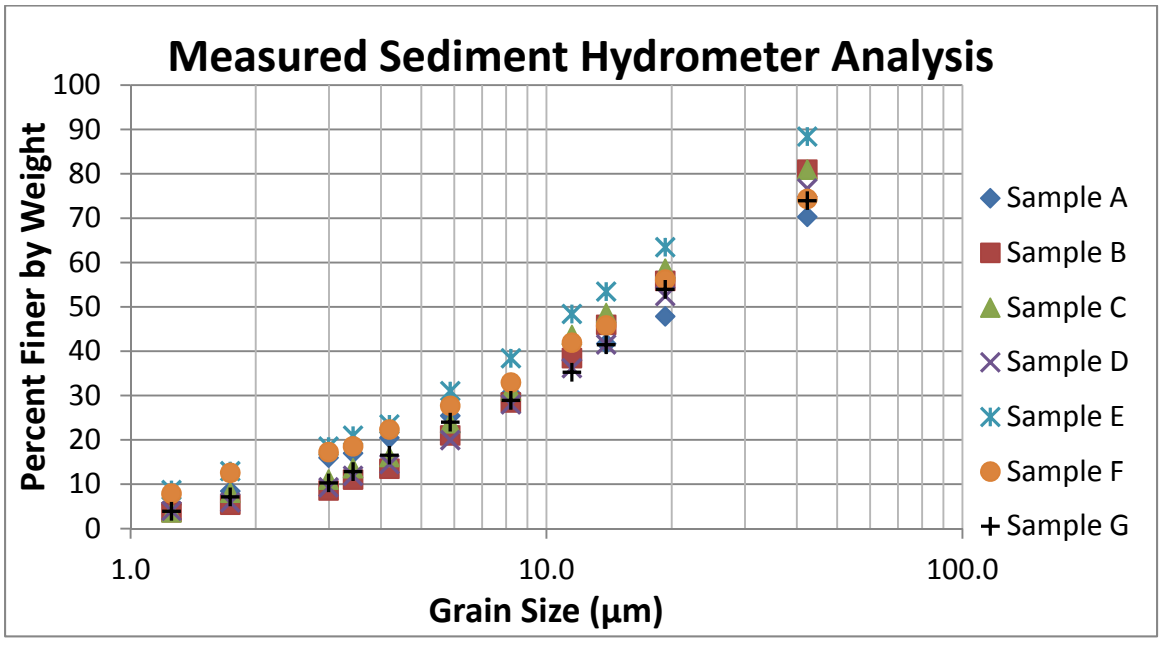

Figure 17. Measured sediment distribution

Table 8. Estimated sediment composition by particle size classification

Sample	Clay (%)	Silt (%)	Sand (%)
A	9	66	25
B	3	74	23
C	5	73	22
D	4	71	25
E	11	74	15
F	11	65	24
G	5	70	25

All seven samples had similar distributions. In each of the samples, the majority of the sediment particles were found to be in the silt range, which is comprised of particles ranging from 4µm to 62µm in diameter (Chang, 1988). The hydrometer measured approximately 80% of the particles to be smaller than 42µm. For these particles in the clay and silt range, Stokes' law was used to calculate the fall velocities (Chang, 1988) as follows:

$$w_s = \frac{gd^2}{18}\left(\frac{\rho_s - \rho}{\mu}\right) \quad [27]$$

where:

W_s = Particle fall velocity, m/s
d = Particle diameter, m
g = Gravitational constant (9.81), $m(s)^{-2}$
ρ_s = Particle density (1922), $kg(m)^{-3}$
ρ = Mass density of fluid (998.2), $kg(m)^{-3}$
μ = Absolute viscosity (1.002×10^{-3}), $N{\cdot}s(m)^{-2}$

Using these velocities, estimated settling times were calculated using an approximate 6ft average pond depth. Figure 18 illustrates the settling times calculated using Stokes' Law for the range of silt and clay particles that were measured by the hydrometer analysis.

The particle settling times were then compared to the adjusted duck pond residence times. To determine the percent of sediment particles expected to settle for various residence times, the settling times shown in Figure 18 were applied to the average of the seven sample grain size distribution measurements in Figure 17. The resulting output, termed average settling efficiency, is shown in Figure 19 and accounts for both the measured particle size distribution and the theoretical particle settling time.

The adjusted duck pond residence times in Table 7 range from 0.2 hours at the pond's peak outlet capacity to 16.6 hours at very low outlet capacity. At peak outlet capacity (0.2-hour residence time), Figure 19 predicts that less than 20% of the measured fraction of sediment yield will settle. Only the large silt and sand particles are expected to accumulate on the bottom of the pond during these large storm events. In contrast, at the pond's lowest modeled output, a maximum of 70% of the measured fraction of sediment yield is expected to settle. This is because during low flow conditions, there is theoretically more time for the particles to settle, but the measured distribution is still very fine.

The particle distribution analysis does not include detailed data for particles in the sand range. This means that the expected settling times were not calculated for particles over 42 μm, which was the largest particle diameter measured by the hydrometer. Therefore, additional detail regarding the percent of particles predicted to settle is not available for duck pond residence times less than 0.6 hours. If available, additional gradation data in the sand range could be used to extend this analysis to provide more detailed predictions at very low residence times, allowing more precise calculations of settling efficiencies below 20%.

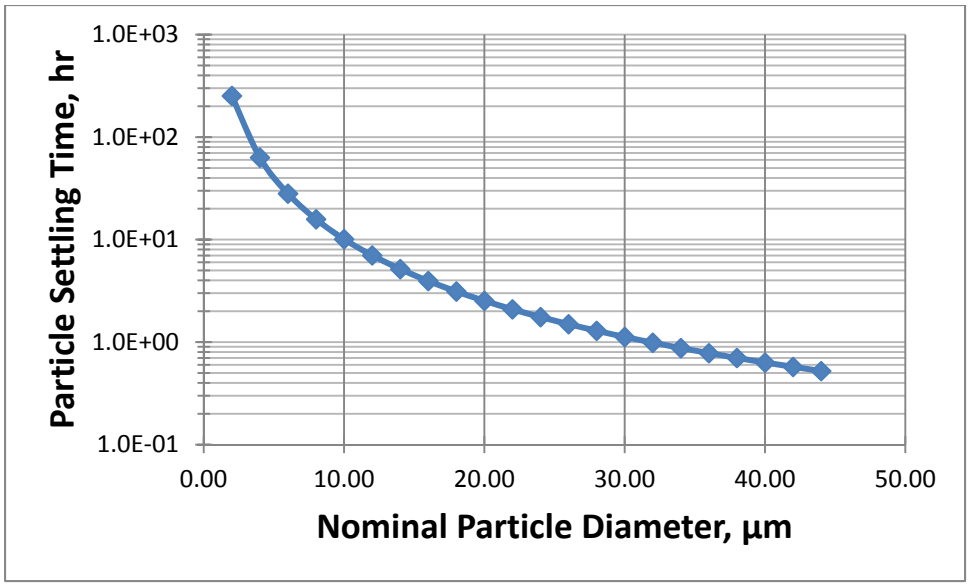

Figure 18. Particle settling time vs. nominal particle diameter

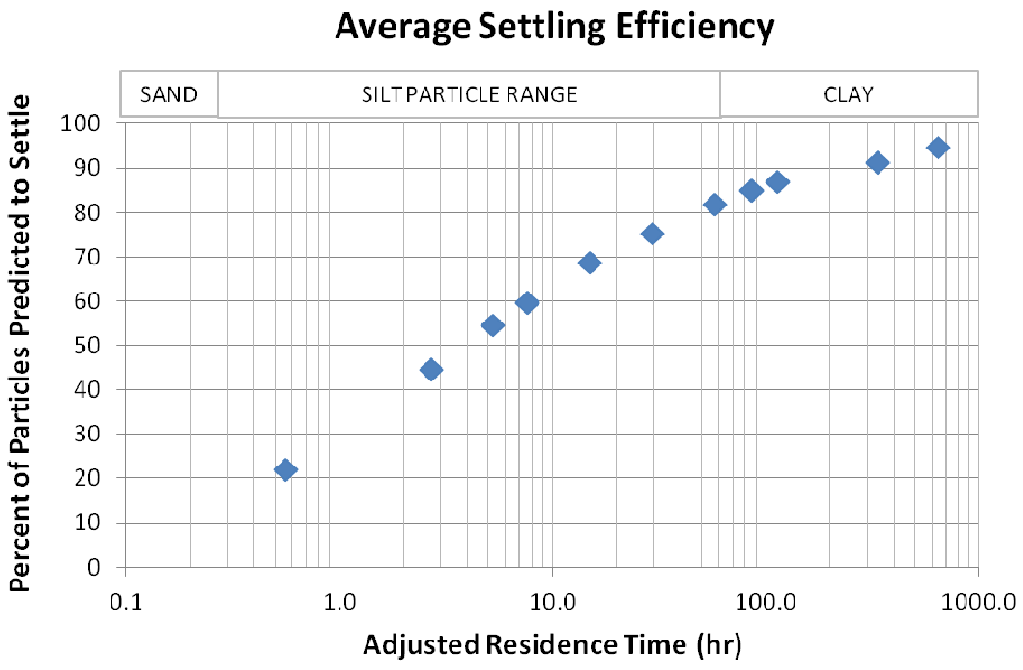

Figure 19. Average particle settling efficiency - Percent of particles predicted to settle vs. the adjusted duck pond residence time.

Before the analysis, it was expected that smaller-diameter particles (clay and small-diameter silt) would not settle because of their high particle setting times. However, the duck pond residence times versus measured particle settling times analysis

indicates that a fraction of these unexpected particles did in fact settle in the pond. The presence of settled clay and small-diameter silt particles are likely the result of dead zones, extreme low flow conditions, and/or the undermined pond foundation walls. The pond perimeter foundation walls sit on rotten railroad ties. The failure has caused a small amount of soil material from the pond perimeter to detach and deposit in the pond. Compared to yield from the watershed, it is estimated that material detached from the pond failure locations contributes a relatively small fraction of the accumulated sediment.

The accumulated sediment samples collected in the duck pond only account for the fraction of the yield that settled. This study does not account for the fraction of sediment that remained suspended and continued downstream. Based on the results of the settling time analysis, this limitation is expected to skew the measured distribution toward larger particles. Because they are more likely to settle, large particles that reach the pond are more likely to end up in the sediment samples collected. In contrast, some of the small particles are expected to remain entrained, and therefore small particles are likely under-represented in the sediment samples relative to the actual sediment yield distribution.

A hydraulic model of the duck pond combined with suspended sediment measurements collected for each storm event during the accumulation period is needed to adequately measure the fraction of yield deposited in the duck pond. For each storm event, the hydraulic model could calculate a pond hydrograph and determine the outlet flowrates over time. This information could then be used to more accurately determine the duck pond residence times for each storm event, which

can be compared to suspended sediment concentrations. Without the additional information of event-by-event based flowrates, results from this study can only speculate how the RUSLE/SEDD model compares to the actual sediment accumulations in the Emory & Henry College duck pond. This approximation has implications in the following interpretation of measured vs. modeled sediment yield results.

3.5. Model vs. Measured Results Interpretation

The total sediment yield predicted at the duck pond was 1,076 $t \cdot (yr)^{-1}$, which utilized the calculated rainfall-runoff erosivity factor R of 161. The model predicted approximately 6 times the accumulation of 170 $t \cdot (347\ days)^{-1}$, or 179 $t\ (yr)^{-1}$, measured at the duck pond.

The numerical sediment model results deviated significantly from the measurement-based estimation of deposited sediment. This variation can be attributed to uncertainties in both the RUSLE/SEDD model and the estimation of deposited sediment from physical surveys. The entrainment of sediment reaching the pond may also contribute to the discrepancy between the measured and modeled results. It is likely that the RUSLE/SEDD model predicted the sediment yield more accurately than the 6x ratio implies. Based on the analysis in Section 3.4.2, the RUSLE/SEDD model may have over-predicted the sediment yield by a factor less than 6x. As described above, an event-based hydraulic pond model would be required to more precisely quantify this number. This analysis should be interpreted as a qualitative comparison which shows that the RUSLE/SEDD model over-predicted sediment yield by a significant amount but was within an order of magnitude of the actual value.

In the literature, some authors maintain that the RUSLE model may have a fundamental tendency to over-estimate erosion in some cases (Svorin, 2003). Some have attributed this to RUSLE's origins as an empirical erosion prediction tool for agricultural lands, but there exist many credible references in which RUSLE was applied successfully to diverse watersheds with accurate results (Tiwari et al., 2000). Using GIS to apply the RUSLE and SEDD models at the watershed scale introduces additional uncertainty. Discussion on these limitations is provided in Section 4.2.

The measurement of deposited sediment is predicated on the assumption that a known percentage of the sediment delivered to the pond is deposited there. The sediment measurement only accounted for the amount of sediment that settled in the pond and did not account for the amount of sediment that continued downstream. There are three known springs which inject a large quantity of groundwater into the pond. These springs likely prevent sedimentation by re-suspending particles that would otherwise settle in less turbulent conditions. Additionally, the pond's small size and outlet structure result in a short residence time, which further reduces the amount of accumulated sediment. With this in mind, it is expected that the model would over-predict the measured value, but a true comparison to modeled versus measured yield is not possible without quantifying the fraction of the yield that continued past the pond. This is an opportunity for future study.

Chapter 4. Discussion

4.1. Assumptions & Limitations

Uncertainty exists in both the modeled yield and the measured accumulation. Identifying assumptions and limitations is important when interpreting the results of this and other similar studies.

4.1.1. Grid Size Selection

For model implementation in GIS, a watershed is broken into discrete morphological units (grid cells), the size of which is user defined. Similar studies selected cell sizes ranging from 10 - 30 meters (Svorin, 2003) This Study used a cell size of 100 ft (30.48 m) in part because of cell sizes selected from similar studies and also because the selected scale is similar to the RUSLE experimental plots and reference length of 72.6 feet (Wischmeier & Smith, 1978). Svorin, 2003 found that increasing the grid cell size resulted in increased erosion rates "...because the cell size is used as slope length, which means that the choice of grid-cell size has an influence on modeled erosion rates".

It is important to consider the computing capabilities of available hardware and software when choosing a cell size. For large watersheds, a small cell size may overwhelm the software. Even for this project, which considered a relatively small watershed with a 100 foot square cell size, ArcGIS frequently crashed, failed to compute raster calculations, and by the end of the project, could no longer save changes to the file. With technological growth in GIS software development, over time these types of issues should be resolved.

4.1.2. Soil Erodibility Factor Assumptions

Soil erodibility information was not available for the Udorthents land complex, which was found on the Emory & Henry College campus. Udorthents is an urban land complex that describes soils affected by manmade land disturbance activities. As described in Section 3.1.2, an assumed median value of 0.32 was assigned to this land complex. Because the Udorthents complex only contributed 0.08% to the total watershed area, the assumed value is not expected to significantly affect the modeled results in this study. However, this issue does illuminate one of the challenges, and potential overreaching applications, in applying the RUSLE model to urban watersheds. Assigning assumed K_f values to urban lands without the benefit of geotechnical explorations may result in uncertainty in the erosion prediction model. If RUSLE is to be applied to urban watersheds, K_f equivalent values for urban land development would need to be established.

4.1.3. Cover Management Factor Assumptions

Estimation of C values based on aerial photography and common regional land use practices represents an important step in the practical implementation of any RUSLE model based on publicly-available information. In the absence of detailed information about current and historical farming practices, such as plow methods or crop rotations, C values must be estimated using the rationale described above. For example in this study, it was impractical to interview each farmer in the watershed to determine the soil loss ratio factors, particularly due to the local sensitivity to sedimentation issues in the duck pond. The College spends approximately $30,000 every 2-3 years to dredge the pond.

This process of estimation introduces a potential source of error. Error is expected to be larger in the cropland subareas than in the forest or grassland subareas, which have a much smaller range of reasonable variation. To reduce the amount of error, the Washington County Extension Agent was contacted to confirm cropping systems on the agricultural croplands. Average annual soil loss was calculated for two different schemes to determine the C value sensitivity. Table 9 summarizes the results. In scheme 1, the cropland was assumed to be either corn or soybeans. In scheme 2, which was used to produce the results in this study, the cropland was assumed to be corn or corn followed by a small grain cover crop. Changing the assumed cropland C values by 10 % resulted in an 18 % change in the cropland average annual soil loss values. This indicates how sensitive the RUSLE model is to variations in C value.

Table 9. Average annual soil loss sensitivity to changes in C value, $t(ac \cdot yr)^{-1}$

Land Cover	Scheme 1		Scheme 2	
	C	A	C	A
	-	$t \cdot (ac \cdot yr)^{-1}$	-	$t \cdot (ac \cdot yr)^{-1}$
Forested	0.001	0.5	0.001	0.5
Grassland	0.014	2.2	0.012	2.0
Urban	0.030	4.9	0.030	4.9
Cropland	0.323	35.3	0.293	29.9
Harvested Forest	0.200	84.6	0.200	84.6

Ultimately, any practical implementation of RUSLE on the watershed scale will involve the C value estimation methodology presented in this study. The C value sensitivity analysis suggests that assuming values for C has the potential introduce uncertainty in the model results.

4.1.4. Beta Value Assumptions & Sensitivity Analysis

The β value is a basin specific parameter used in the sediment delivery ratio calculation according to Equation 4. A value of 0.0186 was assumed for this study as discussed in Section 3.2.1. To test the sensitivity of this assumption, the sediment yield was calculated using three different β values contained in Table 10. β values of 0.0165 and 0.0201 correspond to the range presented in Ferro & Porto, 2000. A 22 % increase in β resulted in a 39 % increase in sediment yield.

Table 10. Sediment yield sensitivity to changes in beta value, $t \cdot (yr)^{-1}$

Sediment Yield $t \cdot (yr)^{-1}$		
β = 0.0165	β = 0.0186	β = 0.0201
1,313	1,076	945

The β value has the greatest influence on the SDR as the travel time increases. For this study, not a lot of sediment originates from the portion of the watershed with higher travel times, therefore the beta value was not expected to greatly influence the results of this study. For other watersheds with significant erosion in the outlying portions of the watershed, the beta value could significantly influence the sediment yield results.

4.1.5. Sediment Measurement Limitations

Following the procedures described in Section 3.4.1, the accumulated sediment volume was estimated using information from a topographic survey. Physical data collection limitations, including the inability to collect information in the center of the pond, and others introduce uncertainty in the topographic sediment measurement.

The dense saturated sediment prevented the survey crew from reaching the pond center. With every step, the survey crew sunk down into the sediment making it difficult to maneuver. It was impossible to reach certain parts of the pond for fear of losing equipment or getting stuck in the sediment. The 3-dimensional surfaces created by AutoCAD Civil3D were generated by triangulation between survey points. Without topographic data for the pond center, the interpolation spacing in this area was greater than the rest of the pond, which reduced the surface accuracy at the pond center.

The data collection involved pushing the survey rod deep into the sediment to collect information on the bottom surface. Folk knowledge from the College Facilities Staff indicated the pond bottom was solid bedrock. A limitation to the collection method was that the surveyor was unable to directly observe the geographic features of the bottom surface. This meant the surveyor relied on how the rod "felt" when it hit bottom. For most of the survey points, the surveyor was confident that bedrock was found. There are also uncertainties in the bottom surface survey because the points may have hit pinnacle rock or a densely compacted sediment that was not actually bedrock. This uncertainty indicates the measurement may have underestimated the actual sediment volume.

The survey rod was pushed as far down into the sediment as possible, but in some cases the data collection was limited by the rod length. It was estimated that only a few of the survey points were influenced by this limitation where the sediment depth was actually greater than that measured by the survey. This limitation also indicates that the measurement may have underestimated the actual sediment volume.

Topographic information below the water surface elevation and sediment accumulation in the springhouse foundation area was not collected by the topographic survey. For the springhouse foundation area, sediment accumulation and volume characteristics were approximated through visual inspection and comparison to accumulations measured in the main pond.

4.2. Model Implementation in GIS

4.2.1. Watershed Scale Application

A limitation to applying the RUSLE and SEDD models at the watershed scale is that each morphological unit is assumed to be homogenous. ArcGIS raster calculations produce a single value for each grid cell. For example, when the RUSLE A value was calculated, a single A value was assigned to each grid cell. This limitation means that heterogeneity within each morphological unit is ignored - the grid cell size then becomes the resolution.

When applying the field-scale RUSLE model using a spatially distributed approach, it is important to consider the calculated and input data accuracies to properly interpret the modeled results.

4.2.2. Data Sources & Accuracy

Each of the data sources used in this study introduces uncertainty due to the quality and resolution of the dataset. The 2007 orthophotography (aerial imagery) has a scale of 1:2,400 with a 1-foot resolution (http://www.vita.virginia.gov). A digital terrain model was created from masspoints and breaklines to orthorectify the 2007 orthophotography. Topography from this digital terrain model was used to create the

digital elevation model in ArcGIS. According to the terrain model metadata, the vertical accuracy of masspoints and breaklines is about 2.5 feet. The topographic resolution is variable across the dataset. In general, the model is accurate enough to produce 5-foot contours.

The accuracies described above provide context for interpreting the results of this study. The topographic resolution used to create the digital elevation model greatly affects the accuracy of the modeled results. Most of the modeled raster calculations, such as the S and L factors, originated from the digital elevation model. The accuracies described above provides context for interpreting the results.

4.2.3. GIS Calculation Methods

ArcGIS was used to perform the calculations described in Chapter 2. Certain raster calculation tools, such as the slope tool, topo to raster tool, flow accumulation tool, and flow direction tool, introduced error in the erosion and yield prediction models.

The slope tool was used by the RUSLE model to calculate the S factor. The slope function calculates the maximum rate of change, or steepest downhill decent, in value from the cell in question to its eight adjacent neighbors (http://resources.arcgis.com/en/help). This calculation technique introduces error for grid cells with slope variation, particularly for cells that only have a small portion of steep topography. In this case, while most of the cell is relatively flat, the steeper portion will dominate the calculation and introduce error.

The topo to raster tool was used to create the digital elevation model from the topographic contours. "The Topo to Raster tool is an interpolation method

specifically designed for the creation of hydrologically correct" DEMs (http://resources.arcgis.com/en/help). It is based on the ANUDEM program developed by Michael Hutchinson (Hutchinson, 1988, 1989, 1996, 2000, and Hutchinson et al., 2011). This method is based on an iterative finite difference interpolation technique (http://resources.arcgis.com/en/help). The accuracy of the topo to raster tool is highly depended on the quality of the input topography. More detailed information regarding the topo to raster calculation limitations can be found in Hutchinson, 1988, 1989, 1996, 2000; Hutchinson & Gallant, 2000; Hutchinson et al., 2011; and Wahba, 1990.

The flow accumulation tool was used in the L factor calculation. "The flow accumulation tool calculates accumulated flow as the accumulated weight of all cells flowing into each downslope cell in the output raster ... and the value of cells in the output raster is the number of cells that flow into each cell" (http://resources.arcgis.com/en/help). As described in Section 3.1.3, the L factor is a length-based calculation that must be transformed into an area-based calculation for implementation at the watershed scale using ArcGIS. Uncertainty associated with this factor is most likely from the calculation transformation and less likely from the ArcGIS flow accumulation calculation.

The flow direction tool was used in the SEDD travel time and L factor calculations. The flow direction tool classifies the flow across a grid cell as one of eight directions. "This approach is commonly referred to as an eight-direction (D8) flow model and follows an approach presented in Jenson and Domingue, 1988 (http://resources.arcgis.com/en/help). Most obviously, the tool is limited by the

constraint to eight flow directions, but it is also has limitations inherent in the calculation. "The direction of flow is determined by the direction of steepest descent, or maximum drop, from each cell" (http://resources.arcgis.com/en/help). Like the slope tool, the flow direction calculation introduces error for grid cells with slope variation. However, it is likely that these errors are randomly distributed in direction and therefore have a tendency to cancel each other out when the raster gradient map is used to calculate the overland flow path for each cell.

The zonal statistics calculator was used to perform statistical calculations to report the results of this study. The calculator was used to determine the total sediment yield by summing the individual sediment yields for each grid cell across the watershed. It was also used to calculate mean value statistics by land cover category. Little error was expected from the zonal statistics calculations.

4.3. Similar Study Comparison

This project follows closely the work of Fernandez et al., 2003. Comparing the results of this project to those of Fernandez et al., 2003 provides useful context. Table 11 provides a summary of the RUSLE results for both projects. The average annual soil loss rates calculated in this study were between 3 and 4 times higher than those calculated by Fernandez et al., 2003. A comparison of the results reveals that the average annual soil loss differences are primarily attributed the R, LS, and C factors. The watershed in this study is located in a climate that experiences more precipitation and has steeper slopes. The larger R and LS factors contributed to the higher A values calculated by the RUSLE model. Also, as discussed in Section 4.1.3, C factor assumptions can greatly influence the modeled erosion rates. This study

assumed higher values for grassland and cropland, which also explains why the A values in this study were higher than those calculated by Fernandez et al., 2003. This comparison demonstrates how sensitive the RUSLE model is to spatial variability and watershed-specific characteristics (rainfall, topography, land use, and soil characteristics), even for similar studies.

Table 11. RUSLE results comparison to Fernandez et al., 2003

RUSLE Results - This Study									
Land Cover	**Area**	**Area %Total**	**R**	**Kf**	**LS**	**C**	**P**	**A**	**A % Total**
	ac		*	**	-	-	-	$t\cdot(ac\cdot yr)^{-1}$	
Forested	372	31%	161	0.37	9.1	0.001	1.0	0.5	1.6%
Grassland	282	24%	161	0.34	3.1	0.012	1.0	2.0	4.4%
Urban	305	26%	161	0.35	2.8	0.030	1.0	4.9	11.7%
Cropland	172	14%	161	0.34	2.8	0.293	0.7	29.9	40.3%
Harvested Forest	64	5%	161	0.36	7.1	0.200	1.0	84.6	42.1%

RUSLE Results - Fernandez et al. 2003									
Land Cover	**Area**	**Area %Total**	**R**	**Kf**	**LS**	**C**	**P**	**A**	**A % Total**
	ac		*	**	-	-	-	$t\cdot(ac\cdot yr)^{-1}$	
Forested	22,410	16%	141	0.38	3.4	0.001	1.0	0.2	0.5%
Grassland	38,452	28%	135	0.36	3.4	0.003	1.0	0.5	2.5%
Urban	269	0.2%	130	0.34	1.2	0.030	1.0	1.6	0.1%
Cropland	76,190	55%	129	0.34	1.9	0.128	0.9	9.6	96.9%
Harvested Forest	-		-	-	-	-	-	-	-

The watershed modeled by Fernandez et al., 2003 was much larger than the watershed analyzed in this study and the agricultural cropland occupied a much greater percentage of the watershed - 55% cropland versus 14% cropland in the duck pond watershed. Another notable difference is that the duck pond watershed included a section of harvested forest, which contributed significantly to both the eroded sediment and sediment yield. The harvested forest accounted for 5% of the total duck

pond watershed area and contributed 42.1% to the predicted average annual erosion. Due to the watershed characteristics, namely the cells with long travel times, only 22% of the total sediment yield originated from this land category.

Table 12 provides a summary of the SEDD results for both projects. The SDR values for forestland, grassland, and cropland are much smaller in this study compared to those calculated by Fernandez et al., 2003. This difference greatly influenced the yield estimates. For example, the urban land in this study was relatively close to the duck pond, hence why it had the highest SDR value of any land use category in the watershed. In the Fernandez et al., 2003 study, the urban land was located in one of the most geographically distant areas of the watershed (Lawyers Creek Watershed). In other words, the urban land was far from the study point. This, coupled with the fact that the urban land only contributed 0.2% to the total Lawyers Creek watershed, is the reason why the urban land in the Fernandez et al. 2003 study contributed insignificantly to the yield.

Yield estimates for forestland and grassland were similar. Most of the sediment yield in the Fernandez et al., 2003 study came from the cropland, which was also the case in this study.

Table 12. SEDD results comparison to Fernandez et al., 2003

SEDD Results - This Study				
Land Cover	**Area**	**SDR**	**Y**	**Y * % Total**
	ac	-	$t \cdot (ac \cdot yr)^{-1}$	%
Forested	372	0.07	0.02	0.6%
Grassland	282	0.09	0.11	2.9%
Urban	305	0.26	0.97	27.5%
Cropland	172	0.11	2.93	46.9%
Harvested Forest	64	0.06	3.72	22.0%

SEDD Results - Fernandez et al., 2003				
Land Cover	**Area**	**SDR**	**Y**	**Y * % Total**
	ac	-	$t \cdot (ac \cdot yr)^{-1}$	%
Forested	22,410	0.32	0.08	0.8%
Grassland	38,452	0.45	0.28	4.5%
Urban	269	0.14	0.21	0.0%
Cropland	76,190	0.26	2.94	94.7%
Harvested Forest	-	-	-	-

4.4. Erosion Mitigation & Conservation Strategies

Using information in this study, erosion control strategies can be implemented throughout the watershed to decrease the amount of eroded sediment and ultimately the sediment yield reaching the duck pond.

Knowing that the sediment yield most likely originates from the section of harvested forest and specific agricultural croplands, strategies targeting these specific locations will have the greatest impact on sediment yield. The College could work with farmers to implement less erosive farming practices or even alternative cropping systems that are more economical than periodic dredging. For example, some of the croplands identified as corn did not plant ground cover after harvest - others did. The farms that did follow the corn harvest with a small grain cover crop were assigned a C value 30 % lower than the farms that did not.

For the section of harvested forest, it is recommended that an erosion and sediment control plan be developed as per the Virginia Erosion and Sediment Control Handbook (VESCH). Using these guidelines, erosion control strategies would most likely include sediment trapping and diversion practices, such as sediment traps, sediment basins, diversion dikes, and silt fence.

Chapter 5. Conclusions

This project identified erosion sources within the Emory & Henry College duck pond watershed and predicted the annual sediment yield expected to accumulate at the pond. The duck pond watershed is approximately 1,194 acres consisting of 26 % low density urban land, 14 % agricultural farmland, 24 % grassland and pasture, 31 % forestland, and 5 % harvested forestland with highland slopes approaching 32 degrees.

The Revised Universal Soil Loss Equation was used to identify erosion hotspots and to estimate gross erosion across the watershed. The Sediment Delivery Distributed model was then used to determine the total sediment yield at the duck pond. In ArcGIS the RUSLE and SEDD models were applied using a raster grid of approximately 5,200 discrete morphological units, or grid cells, and calculating the factors for each cell. The total sediment yield predicted at the duck pond was 1,076 $t \cdot (yr)^{-1}$, which utilized the calculated rainfall-runoff erosivity factor R of 161.

The predicted value was then compared to the actual sediment volume measured by a topographic survey on September 11, 2012. The survey determined that 210 yd^3 of saturated sandy silt accumulated in the duck pond between October 2011 and September 2012. The sediment volume was estimated to have a dry weight of 170 tons.

To interpret the sediment volume measurement, theoretical duck pond residence times for various flow scenarios were compared to the average discrete particle settling times of the accumulated sediment. Seven (7) duck pond sediment samples were collected on May 7, 2013 to determine the particle size distribution of the accumulated sediment and to ultimately calculate the particle settling times. At peak outlet capacity (0.2-hour

residence time), it was predicted that less than 20% of the measured fraction of sediment yield is expected to settle. In contrast, at the pond's lowest modeled output, a maximum of 70% of the measured fraction of sediment yield is expected to settle.

The accumulated sediment samples collected in the duck pond only account for the fraction of the yield that settled. This study does not account for the fraction of sediment that remained suspended and continued downstream. This finding supports the relationship between the modeled sediment yield calculation of 1,076 $t \cdot (yr)^{-1}$ and the field-measured sediment accumulation of 170 $t \cdot (347 \text{ days})^{-1}$. The modeled values are expected to over predict the field-measured accumulation due to the short pond residence time, particle sediment velocities, and more than likely, the turbulent spring water bubbling up from the pond bottom as well as from RUSLE's potential to over-estimate erosion.

It is likely that the RUSLE/SEDD model predicted the sediment yield more accurately than the 6x ratio implies. An event-based hydraulic pond model coupled with suspended sediment measurements would be required to more accurately evaluate the accuracy of the RUSLE/SEDD model. The analysis presented in this study should be interpreted as a qualitative comparison which shows that the RUSLE/SEDD model over-predicted sediment yield by a significant amount but was within an order of magnitude of the actual value.

This project follows closely the work of Fernandez et al., 2003 and shows how RUSLE and SEDD can provide useful information about complex watersheds in a variety of regions. The model was successfully applied to a watershed in Southwestern Virginia,

which had significantly different vegetation, rainfall characteristics, and slopes vs. the Western Idaho watershed analyzed by Fernandez et al. Until an alternative model, such as the WEPP model, is fully vetted and calibrated, the RUSLE is still the most comprehensive erosion prediction model available.

Identification of assumptions and limitations is important when interpreting the results of this and other similar studies. Uncertainty exists in the modeled and measured results as well as in the model implementation in GIS.

The results of this study can be used to develop a water quality improvement plan designed to correct impairments to downstream receiving channels. The results shown in Figure 10, Figure 13, Table 5, and Table 6 identify the sources of erosion and the quantities expected to reach the duck pond. There is no single source, but rather a range of several major erosion contributors (agricultural cropland, urban areas, and portions of harvested forest), which must be addressed in order to solve problems at the duck pond. Emory & Henry College can use the information provided in this study to approach landowners in hopes of implementing erosion control and land management practices in the most critical areas.

REFERENCES

AgriInfo.in. (n.d.). Density of Soil: Bulk Density and Particle Density. In *Soil Science*. Retrieved May 30, 2013, from http://www.agriinfo.in/?page=topic&superid=4&topicid=271.

Blevins, Phil. "Re: Help Interpreting Imagery." Message to Lindsay Lally. 16 May 2013. Email.

Boyce, R. C. 1975. Sediment routing with sediment delivery ratios - present and prospective technology for predicting sediment yield and sources. Publ. ARS-S-40, U.S. Department of Agriculture, Washington, D.C., 61-65.

Chang, H. H.. 1988. Fluvial Processes in River Engineering. Krieger Publishing Company, Malabar, Florida.

Desmet, P.J.J. and G. Grovers. 1996. A GIS procedure for automatically calculating the USLE LS factor on topographically complex landscape units. Journal of Soil and Water Conservation, 51(5): 427-433.

Dissmeyer, G. E. and G.R. Foster. 1980. A guide for predicting sheet and rill erosion on forest land. USDA Forest Service - Southern Region. Atlanta, Georgia.

Draper Aden Associates, Inc. November 17, 2011. Pond and stream improvements report - Emory & Henry College - Emory, VA - Project number B11172B-01.

Fernandez, C., J.Q. Wu, D.K. McCool, and C.O. Stöckle. 2003. Estimating water erosion and sediment yield with GIS, RUSLE, and SEDD. Journal of Soil and Water Conservation, 58(3): 128-136.

Ferro V. and Minacapilli, M. 1995. Sediment delivery processes at basin scale. Journal of Hydrological Science, 40(6): 703-717.

Ferro V. and P. Porto. 2000. Sediment Delivery Distributed (SEDD) Model. Journal of Hydrologic Engineering, 5(4): 411-422.

Finnemore, E. J. and J. B. Franzini. 2002. Fluid Mechanics with Engineering Applications, Tenth Edition. McGraw Hill, New York, NY.

Haan, C.T., B.J. Barfield, and J.C. Hayes. 1994. Design Hydrology and Sedimentology for Small Catchments. Academic Press, San Diego, California.

He, Q., D.E. Walling. 2003. Testing distributed soil erosion and sediment models using ^{137}Cs measurements. Hydrological Processes, 17: 901-916.

Hossain, M. A., M. Alam, D. R. Yonge, R. Dutta. 2005. Efficiency and flow regime of a highway stormwater detention pond in Washington, USA. Water, Air, and Soil Pollution, 164: 79-89.

Hutchinson, M. F. 1988. Calculation of hydrologically sound digital elevation models. Paper presented at Third International Symposium on Spatial Data Handling at Sydney, Australia.

Hutchinson, M. F. 1989. A new procedure for gridding elevation and stream line data with automatic removal of spurious pits. Journal of Hydrology, 106: 211–232.

Hutchinson, M. F. 1996. A locally adaptive approach to the interpolation of digital elevation models. In Proceedings, Third International Conference/Workshop on Integrating GIS and Environmental Modeling. Santa Barbara, CA: National Center for Geographic Information and Analysis. See: http://www.ncgia.ucsb.edu/conf/SANTA_FE_CD-ROM/sf_papers/hutchinson_michael_dem/local.html.

Hutchinson, M.F. 2000. Optimising the degree of data smoothing for locally adaptive finite element bivariate smoothing splines. ANZIAM Journal 42(E): C774–C796.
Hutchinson, M.F. and Gallant, J.C. 2000. Digital elevation models and representation of terrain shape. In: J.P. Wilson and J.C. Gallant (eds) Terrain Analysis. Wiley, New York, pp. 29–50.

Hutchinson, M.F. and Gallant, J.C. 2000. Digital elevation models and representation of terrain shape. In: J.P. Wilson and J.C. Gallant (eds) Terrain Analysis. Wiley, New York, pp. 29–50.

Hutchinson, M.F., Xu, T. and Stein, J.A. 2011. Recent Progress in the ANUDEM Elevation Gridding Procedure. In: Geomorphometry 2011, edited by T. Hengel, I.S. Evans, J.P. Wilson and M. Gould, pp. 19–22. Redlands, California, USA. See: http://geomorphometry.org/HutchinsonXu2011.

Jenson, S. K., and J. O. Domingue. 1988. "Extracting Topographic Structure from Digital Elevation Data for Geographic Information System Analysis." Photogrammetric Engineering and Remote Sensing 54 (11): 1593–1600.

Novotny , Vladimir. 2003. Water quality: diffuse pollution and watershed management, 2nd Addition. J. Wiley, Hoboken, NJ.

Renard, K.G., and G.R. Foster. 1983. Soil conservation: Principles of erosion by water. *In* H.E. Dregne and W.O. Willis, eds., Dryland Agriculture pp. 155-176. Agronomy Monograph No. 23. Am. Soc. Agron., Crop Scien. Soc. Am., Soil Scien. Soc. Am., Madison, WI.

Renard, K.G., G.R. Foster, G.A. Weesies, D.K. McCool, and D.C. Yoder. 1997. Predicting Soil Erosion by Water: A Guide to Conservation Planning with the Revised Universal Soil Loss Equation (RUSLE). U.S. Department of Agriculture-Agriculture Handbook No. 703.

S&ME, Inc. October 10, 2011. Report of geotechnical exploration - Duck pond wall - Emory & Henry College - Emory, VA - S&ME project number 1401-11-098-B.

Svorin, J. 2003. A test of three soil erosion models incorporated into a geographical information system. Hydrological Processes, 17: 967-977.

Thackston, E. L., D. Shields, Jr., and P. R. Schroeder. 1987. Residence Time Distributions of Shallow Basins. Journal of Environmental Engineering, 113: 1319-1332.

Tiwari, A.K., L.M. Risse, and M.A. Nearing. 2000. Evaluation of WEPP and its Comparison with USLE and RUSLE. Transactions of the ASAE, 43(5): 1129-1135.

U.S. Department of Agriculture - National Agricultural Statistics Service (USDA-NASS). 2007. Census of Agriculture - Washington County, VA. Volume 1, Chapter 2: County Level Data.

U.S. Department of Agriculture - Soil Conservation Service (USDA-SCS). 1975. Urban hydrology for small watersheds. Technical Release No. 55. U.S. Department of Agriculture Soil Conservation Service, Washington, D.C.

Wahba, G. 1990. Spline models for Observational data. Paper presented at CBMS-NSF Regional Conference Series in Applied Mathematics. Philadelphia: Soc. Ind. Appl. Maths.

Wischmeier, W.H. 1976. Use and misuse of the universal soil loss equation. Journal of Soil and Water Conservation, 31 (1): 5-9.

Wischmeier, W.H. and D.D. Smith. 1978. Predicting rainfall erosion losses - A guide to conservation planning. U.S. Department of Agriculture - Agriculture Handbook 537. U.S. Government Printing Office, Washington, D.C.

Zhu, T. (n.d.). Some Useful Numbers. In *Useful Links*. Retrieved May 30, 2013, from http://www.stanford.edu/~tyzhu/Documents/Some%20Useful%20Numbers.pdf.